3D PIB and CSF biomarker associations with hippocampal atrophy in ADNI subjects

Liana G. Apostolova[a,b,*], **Kristy S. Hwang**[a,b], **John P. Andrawis**[c], **Amity E. Green**[d], **Sona Babakchanian**[a,b], **Jonathan H. Morra**[b], **Jeffrey L. Cummings**[a], **Arthur W. Toga**[a,b], **John Q. Trojanowski**[e], **Leslie M. Shaw**[e], **Clifford R. Jack Jr.**[f], **Ronald C. Petersen**[g], **Paul S. Aisen**[h], **William J. Jagust**[i], **Robert A. Koeppe**[j], **Chester A. Mathis**[k], **Michael W. Weiner**[l,m], **Paul M. Thompson**[a,b], and **the Alzheimer's Disease Neuroimaging Initiative**

[a] Department of Neurology, David Geffen School of Medicine at UCLA, Los Angeles, CA, United States

[b] Laboratory of Neuro Imaging, David Geffen School of Medicine, UCLA, Los Angeles, CA, United States

[c] Pritzker School of Medicine, University of Chicago, Chicago, IL, United States

[d] Monash University, Victoria, Australia

[e] Department of Pathology and Laboratory Medicine, University of Pennsylvania School of Medicine, Philadelphia, PA, United States

[f] Department of Diagnostic Radiology, Mayo Clinic, Rochester, MN, United States

[g] Department of Neurology, Mayo Clinic, Rochester, MN, United States

[h] Department of Neurosciences, University of California at San Diego, La Jolla, CA, United States

[i] School of Public Health and Helen Wills Neuroscience Institute, University of California. Berkeley, CA, United States

[j] Division of Nuclear Medicine, Department of Radiology, University of Michigan, Ann Arbor, MI, United States

[k] Department of Radiology, University of Pittsburgh, Pittsburgh, PA, United States

[l] Department of Veteran's Affairs Medical Center, San Francisco, CA, United States

[m] Department of Radiology, University of California at San Francisco, San Francisco, CA, United States

Abstract

Cerebrospinal fluid (CSF) measures of Ab and tau, Pittsburgh Compound B (PIB) imaging and hippocampal atrophy are promising Alzheimer's disease biomarkers yet the associations between

[*]Corresponding author at: Mary S. Easton Center for Alzheimer's Disease Research, 10911 Weyburn Ave, 2nd Floor, Los Angeles, CA 90095, United States. Tel.: +1 310 794 2551; fax: +1 310 794 3148. lapostolova@mednet.ucla.edu (L.G. Apostolova).

them are not known. We applied a validated, automated hippocampal labeling method and 3D radial distance mapping to the 1.5T structural magnetic resonance imaging (MRI) data of 388 ADNI subjects with baseline CSF Ab_{42}, total tau (t-tau) and phosphorylated tau (p-tau$_{181}$) and 98 subjects with positron emission tomography (PET) imaging using PIB. We used linear regression to investigate associations between hippocampal atrophy and average cortical, parietal and precuneal PIB standardized uptake value ratio (SUVR) and CSF Ab_{42}, t-tau, p-tau$_{181}$, t-tau/Ab_{42} and p-tau$_{181}$/Ab_{42}. All CSF measures showed significant associations with hippocampal volume and radial distance in the pooled sample. Strongest correlations were seen for p-tau$_{181}$, followed by p-tau$_{181}$/Ab_{42} ratio, t-tau/Ab_{42} ratio, t-tau and Ab_{42}. p-tau$_{181}$ showed stronger correlation in ApoE4 carriers, while t-tau showed stronger correlation in ApoE4 noncarriers. Of the 3 PIB measures the precuneal SUVR showed strongest associations with hippocampal atrophy.

Keywords

Alzheimer's disease; MRI; Magnetic resonance imaging; Imaging; PIB; Amyloid imaging; Abeta; tau; Hippocampus; Atrophy; Biomarkers; ADNI

1. Introduction

Alzheimer's disease (AD), the most common neurodegenerative disorder, is becoming increasingly prevalent among those 65 years and older. Confronted by the grim outlook of tripled AD prevalence by year 2050 (Hebert et al., 2001), scientists are relentlessly working toward earlier diagnosis and disease-modifying strategies that could one day allow primary or secondary disease prevention.

Early and presymptomatic diagnosis can be established by the use of biomarkers. Biomarkers are complementary to the use of clinical outcomes in clinical trials and could one day be used as surrogate endpoints. Good biomarkers should accurately reflect disease progression, predict clinical measures, and demonstrate change with therapeutic interventions that correlate with clinical improvement (Cummings 2009).

Cerebrospinal fluid (CSF) measures of amyloid beta protein (Aβ) and CSF tau, as well as Pittsburgh Compound B (PIB) imaging and hippocampal atrophy are four established AD biomarkers. They all reflect different aspects of AD pathophysiology. Aβ made of 42 amino acids (Aβ_{42}) has been most clearly associated with AD pathogenesis. Aβ is an unstable peptide that tends to polymerize. In its monomeric form, Aβ is soluble and readily measured in the CSF. In AD, increased production, decreased clearance, or a combination of both cause significant increases in the total amount of Aβ. After polymerization, Aβ is sequestered in the brain tissue in the form of amyloid plaques comprised of insoluble fibrillar amyloid. Presumably because of this sequestration, CSF Aβ_{42} levels are low in persons with AD (Blennow and Hampel 2003). Low CSF Aβ_{42} has demonstrated 90%–96% sensitivity and 77%–80% specificity in discriminating AD from cognitively normal elderly (NC) (Andreasen et al., 2001; Galasko et al., 1998; Shaw et al., 2009) and 59%–79% sensitivity and 65%–100% specificity for predicting progression to AD dementia in subjects with mild cognitive impairment (MCI) (Hampel et al., 2004; Mattsson et al., 2009). Also, the Aβ_{42}/Aβ_{40} ratio was recently reported to have 86% sensitivity and 60% specificity for detecting incipient AD in MCI (Brys et al., 2009). Although low CSF Aβ_{42} is a good indicator of AD pathology, CSF Aβ_{42} levels do not correlate well with cognitive measures (Wallin et al., 2006).

Tau is a microtubule-associated stabilizing protein which when hyperphosphorylated detaches from the microtubules and disrupts axonal transport. Similar to Aβ, tau also tends

to aggregate in AD and forms intraneuronal neurofibrillary tangle lesions. Presumably as cells die tau is released into the interstitium and is transported to the CSF. Phosphorylated tau (p-tau) is similarly released from tangles and appears in the CSF. CSF total tau (t-tau) and p-tau are significantly elevated in subjects with AD (Andreasen et al., 2001; Blennow et al., 1995; Clark et al., 2003; Galasko et al., 1998). High CSF t-tau shows 70% sensitivity and 92% specificity in differentiating AD from normal controls (NC) and 83%–86% sensitivity and 56%–90% specificity for predicting progression to AD in MCI (Hampel et al., 2004). p-tau shows 68% sensitivity and 73% specificity in differentiating AD from NC and 73%–84% sensitivity and 47%–88% specificity in diagnosing incipient AD in the MCI stages (Brys et al., 2009; Mattsson et al., 2009). Unlike $A\beta_{42}$, t-tau and p-tau have been associated with cognitive decline (Buerger et al., 2002, 2005; Riemenschneider et al., 2002; Wallin et al., 2006). Research reports by several groups suggest that a combined biomarker measure based on both $A\beta_{42}$ and tau may improve diagnostic accuracy (Galasko et al., 1998; Hansson et al., 2006; Mattsson et al., 2009; Shaw et al., 2009; Visser et al., 2009).

Recent advances in molecular imaging have allowed us to visualize amyloid deposition in vivo, in subjects with AD, using positron emission tomography (PET). Of the available amyloid tracers PIB has been widely used as an AD biomarker although other compounds are also being simultaneously developed (Mathis et al., 2007; Small et al., 2006). The scientific evidence for high cortical PIB retention in AD and low retention in the majority of NC subjects is compelling (Mathis et al., 2007; Mintun et al., 2006). PIB retention in amyloid-rich regions has been reported to be high in postmortem specimens (Ikonomovic et al., 2008; Thompson et al., 2009). A bimodal distribution has been described in MCI with some subjects showing AD-like and others NC-like PIB retention patterns (Kemppainen et al., 2007; Pike et al., 2007). Compared with low PIB retention, high retention conveys substantially higher risk for progression from MCI to AD dementia (87% vs. 7%; Okello et al., 2009) and for cognitive decline in NC (hazard ratio = 4.9; Morris et al., 2009). Although PIB binding shows the expected correlation with cognitive function (Jack et al., 2008b, 2009; Mormino et al., 2009; Pike et al., 2007; Tolboom et al., 2009), longitudinal PIB studies surprisingly have suggested that PIB retention levels off in the dementia stages (Engler et al., 2006). Finally PIB PET has demonstrated better performance than conventional fluorodeoxyglucose (FDG) PET imaging with greater effect sizes and improved spatial resolution for differentiating AD from NC subjects (Ziolko et al., 2006).

Hippocampal atrophy is the most established AD structural imaging biomarker. Hippocampal atrophy is seen in normal aging but is greatly accelerated and steadily progressive in AD (Jack et al., 1997, 1998, 2000). Hippocampal atrophy shows a strong correlation with cognitive decline (de Toledo-Morrell et al., 2000; Fleischman et al., 2005; Mortimer et al., 2004) as well as with AD pathologic markers such as neuronal and neurofibrillary tangle counts and Braak and Braak pathological staging (Bobinski et al., 1995, 1997; Schonheit et al., 2004; Zarow et al., 2005). Using an advanced 3-dimensional (3D) hippocampal mapping technique our group has demonstrated that hippocampal atrophy can predict which MCI subjects would progress to AD during 3-year follow-up (Apostolova et al., 2006b) and that it can detect atrophic changes in cognitively normal elderly 3 years prior to diagnosis of MCI and 6 years prior to diagnosis of AD dementia (Apostolova et al., 2010).

Further advancing biomarker development several research groups have taken the next step toward surrogacy validation (Cummings, 2009) by investigating whether various biomarkers correlate with each other. Region of interest (ROI) studies have reported that CSF p-tau has a stronger association with baseline hippocampal volume and longitudinal volume change compared with CSF t-tau (Hampel et al., 2005; Henneman et al., 2009), while CSF $A\beta_{42}$ shows either a weak (Henneman et al., 2009) or lack of an association (Fagan et al., 2009)

with hippocampal volumetric measures. Negative associations between global PIB retention and ROI-measured hippocampal volume were independently reported in a large NC sample (Storandt et al., 2009), in a relatively large pooled sample consisting of NC, MCI, and AD subjects (Jack et al., 2008b) and in small samples of MCI and NC (Mormino et al., 2009), no association in AD subjects was also reported (Mormino et al., 2009).

Here we aimed to uncover the 3D hippocampal regional associations between several CSF and 1 amyloid imaging biomarker in a large sample from the Alzheimer's Disease Neuroimaging Initiative (ADNI). As CSF tau is thought to be an indicator of neuronal injury we postulated that CSF tau measures will have stronger associations with hippocampal volume and radial distance than CSF Aβ_{42}. We also hypothesized that the brain parenchymal amyloid measure—PIB PET—will show stronger association with structural hippocampal changes than the CSF amyloid measure—a peripheral measure that while being correlated with amyloid load in the brain shows an imperfect correlation. As previous studies have reported effects of ApoE4 genotype on hippocampal volume (Fleisher et al., 2005; Mueller and Weiner, 2009; Mueller et al., 2008; van de Pol et al., 2007), CSF Abeta and PIB binding (Morris et al., 2010) in addition to examining the association in the pooled sample we also modeled the effects in APoE4 carriers and noncarriers separately.

2. Methods

2.1. Subjects

Data used in the preparation of this article were obtained from the Alzheimer's Disease Neuroimaging Initiative (ADNI) database (www.loni.ucla.edu/ADNI). The ADNI was launched in 2003 by the National Institute on Aging (NIA), the National Institute of Biomedical Imaging and Bioengineering (NIBIB), the Food and Drug Administration (FDA), private pharmaceutical companies and nonprofit organizations, as a $60 million, 5-year public-private partnership. The primary goal of ADNI has been to test whether serial magnetic resonance imaging (MRI), positron emission tomography (PET), other biological markers, and clinical and neuropsychological assessment can be combined to measure the progression of mild cognitive impairment (MCI) and early Alzheimer's disease (AD). Determination of sensitive and specific markers of very early AD progression is intended to aid researchers and clinicians to develop new treatments and monitor their effectiveness, as well as lessen the time and cost of clinical trials. The Principle Investigator of this initiative is Michael W. Weiner MD, VA Medical Center and University of California–San Francisco. ADNI is the result of efforts of many coinvestigators from a broad range of academic institutions and private corporations, and subjects have been recruited from over 50 sites across the US and Canada. The initial goal of ADNI was to recruit 800 adults, ages 55 to 90, to participate in the research—approximately 200 cognitively normal older individuals to be followed for 3 years, 400 people with MCI to be followed for 3 years, and 200 people with early AD to be followed for 2 years. For up-to-date information see www.adni-info.org.

The clinical description of the ADNI cohort was recently published (Petersen et al., 2010). Diagnosis of AD was based on the National Institute of Neurological and Communicative Disorders and Stroke and the AD and Related Disorders Association (NINCDS-ADRDA) criteria (McKhann et al., 1984). AD subjects were required to have Mini Mental State Examination (MMSE) (Folstein et al., 1975) scores between 20 and 26 and a Clinical Dementia Rating scale (CDR) (Morris, 1993) score of 0.5–1 at baseline. Qualifying MCI subjects had memory complaints but no significant functional impairment, scored between 24 and 30 on the MMSE, had a global CDR score of 0.5, a CDR memory score of 0.5 or greater, and objective memory impairment on Wechsler Memory Scale – Logical Memory II test (Wechsler, 1987). NC subjects had MMSE scores between 24 and 30, a global CDR of 0 and did not meet criteria for MCI and AD. Subjects were excluded if they refused or were

unable to undergo magnetic resonance imaging (MRI), had other neurological disorders, active depression, or history of psychiatric diagnosis, alcohol, or substance dependence within the past 2 years, less than 6 years of education, or were not fluent in English or Spanish. The full list of inclusion/exclusion criteria may be accessed on pages 23–29 of the online ADNI protocol (see http://www.adni-info.org/Scientists/ADNIScientistsHome.aspx). Written informed consent was obtained from all participants.

As all ADNI subjects had serial 1.5 T MRI images, their inclusion in our analyses was largely determined by the availability of CSF and PIB biomarker data. CSF measures were performed in only a subset of the ADNI subjects while PIB scanning was added to ADNI after the project began, as its promise became more widely recognized. For the CSF/ hippocampal analyses we used all subjects with available baseline CSF Aβ_{42}, CSF t-tau, and CSF p-tau$_{181}$ (i.e., tau phosphorylated at threonine 181) levels as downloaded from the ADNI web site in October 2008. The final CSF biomaker sample consisted of 111 NC, 182 MCI and 95 AD subjects. One hundred ninety-one subjects (49%, 27 NC, 99 MCI, 65 AD) were apolipoprotein E4 (ApoE4) carriers and 197 (51%, 84 NC, 83 MCI, 30 AD) were noncarriers.

For the PIB/hippocampal analyses we used all subjects with available PIB standard uptake volume ratio (SUVR) data from University of Pittsburgh on the ADNI web site in October 2008. The final PIB sample consisted of 19 NC, 62 MCI and 17 AD subjects. As ADNI PIB imaging was added in 2007, the PIB scans analyzed here were acquired at various time points relative to the start of the ADNI study—19 subjects had their PIB scan at the time of their ADNI baseline assessments, 70 subjects at the 12-month, 7 subjects at the 24-month, and 1 subject each at the 6- and 18-month follow-up assessments. The PIB scans were paired with the respective diagnoses and demographic variables in our analyses. Fifty-one subjects (52%, 5 NC, 35 MCI, 11 AD) were ApoE4 carriers and 47 (48%, 5 NC, 35 MCI, 11 AD) were noncarriers.

The study sample of subjects who had both CSF analyses and PIB imaging consisted of 11 NC, 31 MCI and 7 AD subjects. Although PIB was done later relative to the CSF biomarkers the diagnoses of the subjects at baseline and at the time of PIB scans were unchanged. Twenty-seven (56%, 4 NC, 18 MCI, 7 AD) were ApoE4 carriers and 22 (44%, 7 NC, 13 MCI, 2 AD) were noncarriers.

2.2. CSF biomarker data

We downloaded the baseline CSF Aβ_{42}, t-tau and the p-tau$_{181}$ data from the ADNI web site (www.loni.ucla.edu/ADNI) in October 2008. The CSF collection and transportation protocols and procedural details on CSF Aβ_{42}, t-tau and the p-tau$_{181}$ measurements are provided in the ADNI procedural manual posted on www.adni-info.org and in a recent publication by Shaw et al. (2009). Briefly, CSF was collected in the morning, after overnight fast, using a 20- or 24-gauge spinal needle, frozen within 1 hour of collection and transported on dry ice to the ADNI Biomarker Core laboratory at the University of Pennsylvania Medical Center. Aβ_{42}, t-tau and p-tau$_{181}$ were measured using multiplex xMAP Luminex platform (Luminex Corporation, Austin, TX) with Innogenetics (INNO-BIA AlzBio3; Ghent, Belgium) immunoassay kit-based research-use only reagents containing 4D7A3 monoclonal antibody for Aβ_{42}, AT120 monoclonal antibody for t-tau and AT270 monoclonal antibody for p-tau$_{181}$. All CSF biomarker assays were performed in duplicate and averaged. CSF Aβ_{42}, CSF t-tau, CSF p-tau$_{181}$, as well as CSF t-tau/Aβ_{42} and CSF p-tau$_{181}$/Aβ_{42} were used as continuous variables.

2.3. PIB PET data

We downloaded all available University of Pittsburgh PIB SUVR data from the ADNI web site (www.loni.ucla.edu/ADNI/) in October 2008. A detailed description of PIB PET acquisition may be found at www.adni-info.org. The detailed University of Pittsburgh PIB SUVR ROI (region of interest) measurement protocol may be found at www.loni.ucla.edu/twiki/pub/ADNI/ADNIPostProc/UPitt_PIBPET_Analysis.doc. Briefly, ADNI PIB images were collected at 12 ADNI sites. ^{11}C-PIB with minimum 90% radiochemical purity and minimum specific activity of 300 Ci/mmol was synthesized using 1 of 2 methods (Mathis et al., 2007; Wilson et al., 2004). Subjects were injected with 15 ± 1.5 mCi PIB. Dynamic acquisition frames were obtained on a PET scanner 50–70 minutes post injection. A PIB SUVR image was obtained by averaging the individual 50–70 minutes postinjection frames and normalized to the mean PIB retention value of the cerebellar cortex. Each subject's PIB SUVR image was sampled with an automated 14 ROI template including 9 cortical (anterior cingulate, frontal, sensorimotor, lateral temporal, mesial temporal, parietal and occipital cortex, the occipital pole, and the precuneus), 3 subcortical (anterior ventral striatum, thalamus, and subcortical white matter) ROIs as well as the pons and the cerebellum. In our analyses we used the lateral parietal, precuneal, and mean cortical PIB SUVR measures as continuous variables. We decided a priori to use only these regions based on the observed high regional PIB retention in AD subjects. Exploratory analyses with all PIB ROIs with statistical corrections for multiple comparisons could have unnecessarily limited our ability to find significant associations with hippocampal structural changes. The mean cortical PIB SUVR measure was derived by averaging of the 9 cortical ROI measures.

2.4. MRI preprocessing

All subjects were scanned with a standardized high-resolution MRI protocol (www.loni.ucla.edu/ADNI/Research/Cores/index.shtml) on scanners developed by 1 of 3 manufacturers (General Electric Healthcare, Siemens Medical Solutions, and Philips Medical Systems) with a protocol optimized for best contrast to noise in a feasible acquisition time (Jack et al., 2008a; Leow et al., 2006). Raw data with an acquisition matrix of $192 \times 192 \times 166$ and voxel size $1.25 \times 1.25 \times 1.2$ mm^3 in the x-, y-, and z-dimensions was subjected to in-plane, 0-filled reconstruction (i.e., sinc interpolation) resulting in a 256×256 matrix and voxel size of $0.9375 \times 0.9375 \times 1.2$ mm^3. Image quality was inspected at the ADNI MRI quality control center at the Mayo Clinic (in Rochester, MN, USA) (Jack et al., 2008a). Phantom-based geometric corrections were applied to ensure that spatial calibration was kept within a specific tolerance level for each scanner involved in the ADNI study (Gunter et al., 2006). Additional image corrections included GradWarp correction for geometric distortion due to gradient nonlinearity (Jovicich et al., 2006), a "B1-correction" for image intensity nonuniformity (Jack et al., 2008a), and an "N3" bias field correction, for reducing intensity inhomogeneity (Sled et al., 1998). Both the uncorrected and corrected image files are freely available to interested researchers at www.loni.ucla.edu/ADNI.

2.5. Hippocampal segmentation and radial distance analyses

The postprocessed 1.5 3D T1 scans corresponding to the CSF biomarker and the PIB PET data were downloaded and linearly registered to the International Consortium for Brain Mapping (ICBM-53) standard brain template (Mazziotta et al., 2001) using the Minctracc algorithm and 9-parameter (9P) transformation (3 translations, 3 rotations, 3 scales) (Collins et al., 1994). The aligned images were resampled in an isotropic space of 220 voxels along each axis (*x*, *y*, and *z*) resulting in a final voxel size of 1 mm^3. The hippocampi were segmented with our automated machine-learning hippocampal segmentation approach (AdaBoost) which employs the statistical adaptive boosting approach originally proposed by Freund and Shapire (Freund and Shapire, 1997). Using a small training set (in this case 21 subjects—7 NC, 7 MCI and 7 AD) of hippocampi manually defined by an expert (AEG;

intrarater reliability: Cronbach's Alpha = 0.98) as an input, AdaBoost develops statistical rules for classifying future data, i.e., for labeling each voxel in each new image as belonging to the hippocampus or not. The basis for the development of the classification rules are thousands of voxel-specific features, such as image gradients, local curvatures at image interfaces, gray or white matter classification, statistical information on the likely stereotaxic position of the hippocampus, etc. Based on the feature information contained in the positive and negative voxels of the training dataset, AdaBoost develops a set of rules and computes the optimal combination and weighting of these features for accurate segmentation of unknown images by estimating the likelihood that each voxel is inside or outside of the hippocampus. The AdaBoost algorithm has been extensively validated (Morra et al., 2008a, 2008c, 2010) and when labeling new data previously unseen by the algorithm, it agrees with human raters as well as human raters agree with each other (Morra et al., 2008a). We have extensively used AdaBoost in several ADNI and non-ADNI publications (Apostolova et al., 2010; Morra et al., 2008a, 2008b, 2008c).

Once a successful classification model as described above was created, the AdaBoost algorithm was applied to the 2 study imaging samples—the CSF ($n = 388$) sample and PIB ($n = 98$) sample. After converting each hippocampal segmentation into the 3D parametric mesh model, we first computed the medial core for each structure (a 3D medial curve threading down the center of the hippocampus). Next we derived the radial distance from each 3D hippocampal surface point to the medial core (Apostolova et al., 2006a, 2006b; Wilson et al., 2004). This measure essentially represents the thickness of the hippocampal structure at each point on its surface. Hippocampal volumes were also extracted for future analyses.

2.6. Statistical methods

We used 1-way analyses of variance (ANOVA) with posthoc Bonferroni correction for multiple comparisons for continuous variables while examining for diagnostic differences in age, education, and MMSE scores. We used a chi-squared test to determine differences in gender distribution. Pearson's correlation analyses were used to investigate possible associations between hippocampal volume and each biomarker variable. Linear regression models with PIB SUVR as the dependent and mean hippocampal volume as the predictor variable was executed so that we could compare our results with a recent ADNI report relating PIB to hippocampal volume (Mormino et al., 2009).

The 3D associations between CSF and PIB biomarkers and hippocampal radial distance were studied using linear regression. All studied biomarkers show a continuous change from cognitively normal aging to AD, so, to maximize statistical power, we employed linear regression analyses in the pooled sample. Next we investigated these associations separately in ApoE4 carriers and noncarriers. Our linear regression 3D statistical maps were further subjected to multiple comparisons correction by permutation analyses (permuting the predictor variable—in this case the CSF and PIB biomarkers). Using a set-level inference approach (Frackowiak et al., 2007), we defined a final single corrected p-value for each map based on the number of points surviving a particular a priori threshold (set to 0.01 in our analyses). This approach tends to be more sensitive for detecting a distributed pattern of weak effects as opposed to the peak height of the maximum statistic, which is best for detecting a spatially highly concentrated effect.

We next applied map-wise false discovery rate (FDR) correction and derived cumulative p-value cumulative distribution function (CDF) plots from our 3D statistical maps resulting from the linear regression models described above. These CDF plots provide head-to-head comparisons of the strength of the tested associations (in this case between each CSF and PIB biomarker variable and hippocampal radial distance). In other words, the CDF plots

essentially rank the statistical maps in terms of their effect sizes. In the CDF plots the *x*-axis represents any arbitrary *p*-value threshold that can be applied to the map (range between 0 and 1) while the *y*-axis displays the proportion of the statistical map (as a fraction from 0 to 1) that shows effects with significance value below the chosen *p*-value threshold. CDF plots that rise more steeply at the origin have a higher proportion of voxels with effect sizes exceeding the fixed threshold. An additional y = 20× line denotes the threshold that controls the allowed 5% FDR (i.e., the maximum proportion of false positives allowed, by convention, for a map to be declared significant overall). If a given CDF function curves above the y = 20× line and then crosses it again at a more distant point, it means that the corresponding regression map shows statistically significant effect after FDR correction. For maps with greater effect sizes, the CDF crosses the y = 20× line at a higher statistical threshold or critical value, t (i.e., greater extrapolated y value), meaning that a broader range of statistical thresholds can be applied to the data while still allowing greater than 5% of the voxels to remain significant. The critical value, t, represents the highest proportion of voxels that can be shown while still maintaining a certain prespecified FDR (set at the conventional 5% in our analyses); it occurs when the map is thresholded at the highest possible *p*-value that still controls the FDR. We used CDF plots to compare the strength of the associations between hippocampal radial distance, and (1) the 5 CSF biomarkers; (2) the mean cortical, parietal, and precuneal PIB SUVR; and (3) the 3 PIB SUVR measures and CSF $A\beta_{42}$.

3. Results

3.1. Demographic characteristics

The mean demographic characteristics of the diagnostic groups in the CSF ($n = 388$), the PIB ($n = 98$), and combined CSF/PIB ($n = 49$) samples are shown in Table 1. There were no significant age and education differences among the groups in any of the 3 samples. In the CSF ($n = 388$) sample, the MCI group had significantly more males (66%; $p = 0.023$) relative to both the NC (51%) and the AD groups (57%). Sex distribution was not significantly different between the diagnostic groups in the PIB or the combined PIB/CSF sample. As expected, AD subjects had the lowest mean MMSE scores and NC the highest in all samples. There were no subjects who had a change in diagnosis between CSF collection and PIB scanning.

3.2. CSF biomarker analyses

All 5 CSF biomarkers showed significant correlations with hippocampal volume (Table 2) and even more significant associations with hippocampal radial distance in the pooled sample (Fig. 1, Table 2). When split by diagnostic label, significant associations were observed between CSF p-tau$_{181}$ and CSF p-tau$_{181}$/$A\beta_{42}$ and hippocampal volume on the right in the AD group (Table 2). Trend level associations were seen between CSF t-tau and CSF p-tau$_{181}$ and right hippocampal volume and between CSF t-tau, CSF t-tau/$A\beta_{42}$, and CSF p-tau$_{181}$/$A\beta_{42}$, and right hippocampal radial distance in the MCI group (Fig. 2, Table 2). CSF p-tau$_{181}$ showed a trend-level association with left hippocampal radial distance in NC (Fig. 2, Table 2). The correlations between the hippocampal measures and CSF p-tau$_{181}$ and CSF p-tau$_{181}$/$A\beta_{42}$ were stronger in ApoE4 carriers relative to noncarriers (Fig. 3, Tables 3 and 4). In the ApoE4-genotype stratified diagnostic subgroup analyses we had restricted power to detect significant association due to small sample sizes (Tables 3 and 4). Despite these limitations, we found significant associations between CSF p-tau$_{181}$/$A\beta_{42}$ and right hippocampal volume in ApoE4-positive MCI and AD (Table 3). The associations between right hippocampal volume and CSF p-tau$_{181}$ were significant on the right in ApoE4-positive AD and showed a trend on the right in ApoE4-positive MCI (Table 3). These observations were confirmed in the 3D radial distance analyses. The ApoE4-negative diagnostic subgroup volumetric and radial distance analyses (Fig. 4) revealed only trend

level association between CSF t-tau and left hippocampal volume in NC. We used CDF plots to objectively compare and rank the associations between the 5 CSF biomarkers and hippocampal radial distance after applying FDR correction for multiple comparisons. The CDF plots are presented in Fig. 5. Here the t-values correspond to the proportion of the map that remains significant after controlling FDR at 5%. Panel A includes the CDFs of the pooled sample while panel B shows the CDFs in each diagnostic group. In the pooled sample (panel A; $n = 388$) strongest associations were observed for CSF p-tau$_{181}$ and CSF p-tau$_{181}$/Aβ_{42} (t-values = 0.349 and 0.347, respectively), closely followed by CSF t-tau/Aβ_{42} and CSF t-tau (t-values = 0.327 and 0.306, respectively), and finally CSF Aβ_{42} (t-value = 0.278). In the diagnostic subgroup analyzes the only significant association was seen for CSF p-tau$_{181}$ and hippocampal radial distance among NC (t = 0.0004). Among ApoE4 carriers (left column in panel B; $n = 191$) strongest associations with hippocampal radial distance were seen for CSF p-tau$_{181}$ (t-value = 0.06) and CSF p-tau$_{181}$/Aβ_{42} (t-value = 0.035) while among ApoE4 non-carriers (right column in panel B; $n = 197$) CSF t-tau and CSF t-tau/Aβ_{42} showed the strongest effect (t-values = 0.057 and 0.037, respectively).

3.3. PIB SUVR analyses

Significant correlations between hippocampal volume and PIB SUVR were seen bilaterally for the precuneal, average cortical, and parietal PIB SUVR (see Table 5). Similar to the ADNI PIB/hippocampal analyses reported in Mormino et al. (2009) with a sample consisting of 17 NC, 52 MCI, and 15 AD subjects we ran linear regression analysis with mean cortical PIB SUVR as the dependent measure and mean hippocampal volume (left + right/2) as the predictor variable. This model showed a significant linear relationship between the 2 measures (t = −2.55; $p = 0.012$). The precuneal and parietal PIB SUVR linear regression models similarly showed that hippocampal volume is a significant predictor of cortical PIB binding (for precuneal PIB SUVR t = −2.568; $p = 0.009$) and for parietal PIB SUVR t = −2.412 and $p = 0.018$). After splitting the PIB sample by ApoE4 genotype, stronger correlations between PIB SUVR and hippocampal measures were seen in ApoE4 noncarriers (see Table 6).

The 3D significance and correlation maps between PIB SUVR and hippocampal radial distance are presented in Fig. 6. Precuneal PIB SUVR showed significant negative association with the right but not left hippocampal radial distance (right $p_{corrected} = 0.013$). There was a trend level significant association between average cortical PIB SUVR and right hippocampal radial distance ($p_{corrected} = 0.097$). Parietal PIB SUVR failed to show significant associations with hippocampal radial distance. The ApoE4 genotype-stratified 3D significance maps can be seen in Fig. 7. The associations between precuneal PIB SUVR and hippocampal radial distance were significant on the right ($p_{corrected} = 0.05$) among ApoE4 noncarriers ($n = 46$). A trend-level significant association was seen with mean cortical PIB SUVR also on the right in ApoE4 noncarriers ($p_{corrected} = 0.095$). While we found significantly higher PIB SUVR in ApoE4 carriers ($n = 51$) versus, noncarriers (mean cortical PIB SUVR 1.75 vs. 1.54, precuneal PIB SUVR 2.12 vs. 1.74, and parietal PIB SUVR 2.0 vs. 1.75; $p < 0.0001$ for all 3), there were no significant associations between PIB SUVR and hippocampal atrophy in ApoE4 carriers.

Next we used CDF plots to objectively compare and rank the associations between the 3 PIB SUVR measures and hippocampal radial distance. None of the PIB SUVR/hippocampal associations in the pooled or the ApoE4 genotype-stratified analyses survived FDR-correction for multiple comparisons. Most different from the null line corresponding to complete lack of effect was precuneal PIB SUVR in the pooled sample but this should be interpreted with caution, as it did not survive FDR correction.

3.4. Combined CSF Aβ$_{42}$/PIB analyses

These analyses were performed with a sample size of only 49 subjects, i.e., those who had both CSF and PIB examinations. Each biomarker variable was matched with the hippocampal data from the corresponding visit. Relative to the AD subjects from the $n = 388$ CSF sample, AD subjects from the combined CSF/PIB sample were younger ($p = 0.043$) and had lower MMSE scores ($p = 0.002$). In the combined CSF/PIB sample, the NC group had trend level lower CSF Aβ$_{42}$ relative to the NC from the $n = 388$ CSF sample ($p = 0.074$).

We found a trend level association between PIB SUVR and right hippocampal volume (Table 7). The rest of the variables of interest did not show significant associations with hippocampal volume. Fig. 8 shows the 3D significance and correlation maps between CSF Aβ$_{42}$ and each of the 3 PIB SUVR biomarkers and hippocampal radial distance. Following permutation correction for multiple comparisons, trend level associations were seen between right hippocampal radial distance and precuneal PIB SUVR ($p_{corrected} = 0.056$). Similar effects were seen for average cortical PIB SUVR (right $p_{corrected} = 0.07$). Neither parietal PIB SUVR nor CSF Aβ$_{42}$ showed significant associations with hippocampal radial distance. Similarly CSF t-tau and p-tau$_{181}$ showed no significant associations with hippocampal volume and radial distance in the CSF/PIB sample. After map-wise FDR correction, none of the variables showed a significant correlation with hippocampal radial distance.

4. Discussion

A recent expert position paper reviewed the current evidence on imaging and biofluid AD biomarkers and proposed a timely revision of the temporal order of biomarker abnormalities in AD (Jack et al., 2010). The authors posited that the first AD-associated abnormalities are CSF Aβ depletion and cortical amyloid deposition. These events, occurring largely during the cognitively normal stage, precede tau-mediated synaptic and neuronal injury, which are the substrate for hippocampal and cortical atrophy. In full agreement with this model we report stronger associations between hippocampal atrophy and CSF t-tau and p-tau$_{181}$ relative to CSF Aβ$_{42}$ and PIB SUVR.

4.1. CSF biomarkers' correlations with hippocampal volume and radial distance

All 5 CSF markers showed significant relationships to hippocampal volume and radial distance. Strongest associations were seen for CSF p-tau$_{181}$ and CSF p-tau$_{181}$/Aβ$_{42}$ ratio, followed by CSF t-tau/Aβ$_{42}$ ratio and CSF t-tau. CSF Aβ$_{42}$ showed the weakest association with hippocampal volume but unlike the CSF tau measures this association did not hold once the sample was broken down by diagnostic category. These results nicely complement previously reported observations and are consistent with the current model of hippocampal atrophy as a measure of neurodegeneration reflecting neuronal loss secondary mostly to effects of neurofibrillary tangle formation (Jack et al., 2010).

Several research groups have independently investigated the relationship between CSF biomarkers and hippocampal volume (Fagan et al., 2009; Hampel et al., 2005; Henneman et al., 2009) and the power of these CSF measures for differentiating cognitively normal elderly, MCI, and AD subjects (de Leon et al., 2006; Frisoni et al., 2009b). Fagan et al. (2009) reported correlations between CSF t-tau and hippocampal volume of the same magnitude as the ones observed in our pooled sample analyses (NC, Pearson's $r = 0.22$; MCI and mild AD $r = 0.32$) but these failed to reach statistical significance with their study's sample size of 69 NC and 29 in the combined MCI plus mild AD group. While CSF Aβ$_{42}$ also showed no significant correlation with hippocampal volume (NC, Pearson $r = 0.03$ and MCI and mild AD Pearson's $r = -0.004$), subjects with low CSF Aβ$_{42}$ level had

significantly smaller hippocampi relative to those with high CSF Aβ_{42}. Similar to our study, Henneman et al. reported strongest correlations with hippocampal volume for CSF p-tau$_{181}$. The strength of the associations were Pearson's $r = -0.29$ for MCI and $r = -0.25$ for AD (Henneman et al., 2009). Tau phosphorylated at threonine 231 (CSF p-tau$_{231}$) was reported to correlate well with hippocampal volume and atrophy rate while CSF t-tau correlated with baseline volume only (Hampel et al., 2005).

Very recently the ADNI CSF Biomarker Core published the first detailed analyses of the baseline CSF ADNI data (Shaw et al., 2009). They reported that a combination of CSF Aβ_{42}, CSF t-tau, and the apolipoprotein E4 (ApoE4) genotype best predicted AD while CSF t-tau/Aβ_{42} ratio best predicted MCI. Importantly, the same publication also reported an independent diagnostic predictive analysis of AD versus NC. For this classification the authors used the premortem CSF biomarker data of 56 AD subjects all of whom had postmortem examination and diagnostic confirmation and 52 NC. The CSF measure with best diagnostic accuracy of 87% was CSF Aβ_{42} closely followed by CSF t-tau/Aβ_{42} (accuracy of 85.2%), and CSF p-tau$_{181}$/Aβ_{42} (accuracy of 81.5%). The observed best performance of Aβ_{42} however may also be due to the fact that only definite AD (i.e., with pathological confirmation) was allowed in this sample while in the ADNI and any other in vivo study we logically resort to diagnosis of probable AD (without pathologic confirmation) and thus inevitably include some subjects with dementia due to other etiologies.

In line with our hypotheses and in agreement with the studies above, we found that all CSF biomarkers correlated with hippocampal volume. Among the CSF biomarkers, phosphorylated tau showed the strongest association with hippocampal atrophy suggesting that it is a powerful biomarker for neuronal injury. We also found a stronger association between CSF p-tau$_{181}$ and hippocampal atrophy in ApoE4 carriers while a stronger association between CSF t-tau and hippocampal atrophy in ApoE4 noncarriers was present suggesting perhaps a modulating effect of ApoE4 genotype. Past research has also suggested that ApoE4 genotype (Cosentino et al., 2008) and higher CSF p-tau$_{181}$ levels (Ravaglia et al., 2008) are predictive of more rapid cognitive decline.

4.2. PIB SUVR analyses

Of the 3 PIB measures, strongest associations with hippocampal volume and radial distance were seen for precuneal PIB SUVR followed by mean cortical PIB SUVR. To our knowledge this is the first report of regional PIB binding (i.e., precuneal measures, for example, as opposed to mean cortical PIB binding) associations with hippocampal atrophy. It is not surprising to find that precuneal amyloid load has the strongest association with hippocampal structural changes as these 2 areas are strongly connected and functionally related to each other (Dorfel et al., 2009; Laurens et al., 2005; Teipel et al., 2009). A recent study using resting state functional MRI documented decreased connectivity between the precuneus and the hippocampus in subjects with high mean cortical PIB binding (Sheline et al., 2009). Furthermore, the precuneus is also part of the default network, which has been repeatedly found to show abnormal activity in AD subjects (Buckner et al., 2005).

Only a few studies have explored associations between PIB binding and hippocampal volume to date. The strongest association reported comes from Jack et al. who report a Spearman's rho $= -0.48$ ($p < 0.001$) between global cortical PIB retention and hippocampal W score (Jack et al., 2008b). Mormino et al. (2009) recently applied automated hippocampal segmentation using the Freesurfer package (Fischl et al., 2002) to the 1.5 T structural MRI data of 17 NC, 52 MCI, and 15 AD ADNI subjects (total $n = 84$ compared with $n = 98$ in our analyses). While the major focus of the analyses was to relate cortical PIB binding to episodic memory, the authors also investigated associations of mean hippocampal volume

and mean cortical PIB binding. A univariate linear regression model with hippocampal volume as predictor and mean cortical PIB binding as dependent variable showed a significant association ($t = -2.21$, $p = 0.047$). We used a largely overlapping ADNI dataset but employed a different automated hippocampal segmentation technique. Using an identical univariate linear regression model we also found that hippocampal volume is a significant predictor of mean cortical PIB SUVR ($t = -2.364$, $p = 0.02$). We also found an even stronger effect for the precuneal PIB SUVR ($t = -2.578$, $p = 0.011$). Of the 2 studies reporting both PIB and structural hippocampal analyses, 1 did not investigate the direct correlations between these measures. The authors, however, compared mean hippocampal volume between subjects with high and low mean cortical PIB binding and found greater hippocampal atrophy in those with high cortical amyloid load (Storandt et al., 2009). The second study assessed the strength of the associations between regional gray matter atrophy and PIB retention using a voxel-by-voxel approach and reported significant correlations for the hippocampal and amygdalar but not for any of the neocortical regions (Frisoni et al., 2009a). Further building upon this evidence we examined whether hippocampal atrophy associates with PIB retention of one remote region that is functionally connected with the hippocampus—the precuneus (or medial parietal cortex) and another that is not as heavily connected—the lateral parietal cortex.

In the ApoE4 genotype-stratified analyses, despite that higher cortical amyloid burden was observed in ApoE4 carriers, we found a stronger association between all 3 PIB SUVR measures and hippocampal atrophy in ApoE4 noncarriers. Hence it seems plausible that ApoE4 genotype while promoting cortical deposition of fibrillar Aβ does not exert an equally strong influence on hippocampal neurodegenerative changes. In fact the effect of ApoE4 genotype on age of onset of clinical symptoms could be a direct result of more severe cortical amyloidosis resulting in local neurotoxic effects and significant cognitive decline in nonmemory domains. One study reported that ApoE4-positive African American subjects show greater visuospatial deficits relative to ApoE4-negative subjects while the rest of the cognitive domains appeared to be similarly affected (Mount et al., 2009) and another reported an effect on nonmemory function in addition to accelerated memory loss in ApoE4 carriers (Caselli et al., 2009).

4.3. Combined CSF/PIB dataset analyses

The rationale behind this analysis was to compare the correlation between these 2 very different amyloid markers and hippocampal atrophy. Although both CSF Abeta and PIB are labeled "amyloid markers," they measure 2 very different Aβ states: CSF Aβ_{42} is a measure of this peptide in solution (i.e., the product from the cleavage of the amyloid precursor protein molecule by beta and gamma secretase), while PIB labels fibrillar amyloid contained predominantly in the more mature fibrillar plaques. It is not yet known which of these CSF-based markers correlates best with accepted structural measures of neurodegeneration such as hippocampal atrophy. Due to lack of significance, however, our results are inconclusive. As follow-up ADNI CSF biomarker data becomes available and more subjects are scanned with PIB, a consistent matching of the CSF and PIB values and analyses of larger sample sizes will be possible.

To our knowledge this is the largest study investigating the correlations between CSF and PIB biomarkers and hippocampal atrophy. Several strengths and limitations of this study should be acknowledged. Strengths of this study are its large size, the detailed subject assessment, the unified MRI, PIB, and CSF collection protocol across multiple sites and the meticulous data quality control. Additional strengths are the advanced preprocessing and 3D modeling techniques used to map regionally discrete biomarker correlations. As the ADNI was designed to inform decisions about future disease-modifying clinical trials, it uses the very rigorous exclusion criteria typical of clinical trials. As such, it does not represent the

general elderly population and its findings should be generalized with caution. Another relative weakness is the etiologic/pathologic uncertainty in the MCI stage as at least 30% of amnestic MCI subjects have been found to harbor non-AD pathology (Jicha et al., 2006) although etiologic heterogeneity should not be expected to affect a direct biomarker to biomarker correlation across the pooled sample.

Another limitation of our study in terms of statistical rigor for hypothesis testing is that 5 markers for CSF is a relatively large number. These markers are somewhat redundant as the same measures are assessed both separately (amyloid, tau) and combined (ratios of amyloid and tau). Although a strict hypothesis testing approach would mandate that the number of comparisons should be kept to a minimum, essentially, this is a pilot study aiming to generate the maximum possible descriptive information on which of these 5 widely-studied biomarkers correlates best with hippocampal atrophy. In terms of hypothesis testing, the reported correlations are inevitably somewhat exploratory. In addition, there is a strong statistical correlation between all of these candidate biomarkers and some pairings (such as the ratios) are, by definition, derivable analytically from the others. Even so, it appears that p-tau better reflects the neurodegenerative aspects of AD pathology, while t-tau remains the better-studied measure. Some authors advocate using the ratio markers, as they may be most accurate (Fagan et al., 2009). In this article, we report correlations between 2 well established amyloid measures and hippocampal atrophy in the pooled ADNI sample (combining patients with AD, MCI, and controls), yet we also report other correlations within groups split by diagnosis ("disaggregated" analyses). Both types of analysis are complementary, and each has limitations. The pooled analyses aim to determine the association between the chosen disease biomarkers (CSF and PIB measures versus hippocampal atrophy) across the full spectrum from normal aging to dementia. As the whole cohort is arguably a continuum, it is vital to look beyond the diagnostic categories and relate the observed level of atrophy to CSF or PIB biomarker levels. This same correlation may be missed if it is assessed within 1 group only (e.g., NC, MCI, or AD) due to a "restricted range" effect. By running split analyses only, many important correlations will be missed. For instance, the level of brain atrophy correlates well with CSF-derived measures of pathology across the continuum from aging to MCI to AD. But if one subselects a group such as MCI, for instance, or a group of subjects with a very narrow range of disease burden (for instance, AD or NC), it is possible that no such correlation will be detected, due to the restricted range. If the selection criterion (in this case disease stage) for the group correlates with the variable of interest, nearly all the maps would be false negatives due to the truncated range.

Pooled analyses also have limitations. First, one could postulate that correlations between biomarkers in a pooled cohort will tend to show similar patterns to a direct comparison of diagnostic groups or to a correlation of cognitive measures used for making the diagnosis. However, taking together the findings reported in this paper and a previous report by our group (Morra et al., 2009), that seems to not be the case. The pattern of CSF and PIB biomarker correlations with hippocampal atrophy shown here are strikingly different from the between-group comparisons of hippocampal radial distance and the cognitive (MMSE, global and sum of boxes CDR) correlations with hippocampal radial distance in the same ADNI cohort (Morra et al., 2009). Second, if correlation analyses are performed across the full diagnostic continuum in a pooled cohort such as ADNI, any correlations detected may depend somewhat on the proportion of subjects with each diagnosis—in ADNI, this is approximately 1:2:1 for AD:MCI:NC. In other words, part of the range of cognitive decline may be oversampled. In ADNI, the oversampling of MCI is deliberate, but it may not reflect a representative sampling of all subjects of a certain age. As such, any correlations with the atrophy in ADNI may not be detected in the same degree in other population studies with different proportions of subjects, or within diagnostic subcategories. For that reason, both

pooled and split analyses have value for understanding the cognitive and pathological correlates of atrophy.

Hippocampal atrophy is arguably the most established imaging biomarker in AD. It powerfully links with disease progression, correlates well with memory loss and global cognitive decline, as well as with AD pathologic burden. In this paper we have successfully documented significant correlations between CSF and PIB biomarkers and hippocampal atrophy in the expected direction. However, to establish hippocampal atrophy as a clinical trial biomarker and surrogate measure we will now need to demonstrate change in hippocampal atrophy rate under the influence of a successful therapeutic intervention and a strong correlation with clinical improvement or stabilization.

The modulation effect of ApoE4 genotype on the association between hippocampal atrophy and PIB retention is another interesting finding and supports the hypothesis that ApoE4-positive subjects have a more aggressive amyloid-driven endophenotype with somewhat different morphologic expression compared with ApoE4-negative subjects.

Acknowledgments

References

Andreasen N, Minthon L, Davidsson P, Vanmechelen E, Vanderstichele H, Winblad B, Blennow K. Evaluation of CSF-tau and CSF-Abeta42 as diagnostic markers for Alzheimer disease in clinical practice. Arch Neurol 2001;58:373–379. [PubMed: 11255440]

Apostolova LG, Dinov ID, Dutton RA, Hayashi KM, Toga AW, Cummings JL, Thompson PM. 3D comparison of hippocampal atrophy in amnestic mild cognitive impairment and Alzheimer's disease. Brain 2006a;129:2867–2873. [PubMed: 17018552]

Apostolova LG, Dutton RA, Dinov ID, Hayashi KM, Toga AW, Cummings JL, Thompson PM. Conversion of mild cognitive impairment to Alzheimer disease predicted by hippocampal atrophy maps. Arch Neurol 2006b;63:693–699. [PubMed: 16682538]

Apostolova LG, Morra JH, Green AE, Hwang KS, Avedissian C, Woo E, Cummings JL, Toga AW, Jack CR, Weiner MW, Thompson PM. Automated 3D mapping of baseline and 12-month associations between three verbal memory measures and hippocampal atrophy in 490 ADNI subjects. Neuroimage 2010;15:488–499. [PubMed: 20083211]

Apostolova LG, Mosconi L, Thompson PM, Green AE, Hwang KS, Ramirez A, Mistur R, Tsui WH, de Leon MJ. Subregional hippocampal atrophy predicts Alzheimer's dementia in the cognitively normal. Neurobiol Aging 2010;31:1077–1088. [PubMed: 18814937]

Blennow K, Hampel H. CSF markers for incipient Alzheimer's disease. Lancet Neurol 2003;2:605–613. [PubMed: 14505582]

Blennow K, Wallin A, Agren H, Spenger C, Siegfried J, Vanmechelen E. Tau protein in cerebrospinal fluid: a biochemical marker for axonal degeneration in Alzheimer disease? Mol. Chem Neuropathol 1995;26:231–245.

Bobinski M, Wegiel J, Tarnawski M, Bobinski M, Reisberg B, de Leon MJ, Miller DC, Wisniewski HM. Relationships between regional neuronal loss and neurofibrillary changes in the hippocampal formation and duration and severity of Alzheimer disease. J Neuropathol Exp Neurol 1997;56:414–420. [PubMed: 9100672]

Bobinski M, Wegiel J, Wisniewski HM, Tarnawski M, Reisberg B, Mlodzik B, de Leon MJ, Miller DC. Atrophy of hippocampal formation subdivisions correlates with stage and duration of Alzheimer disease. Dementia 1995;6:205–210. [PubMed: 7550600]

Brys M, Pirraglia E, Rich K, Rolstad S, Mosconi L, Switalski R, Glodzik-Sobanska L, De Santi S, Zinkowski R, Mehta P, Pratico D, Saint LLA, Wallin A, Blennow K, de Leon MJ. Prediction and longitudinal study of CSF biomarkers in mild cognitive impairment. Neurobiol Aging 2009;30:682–690. [PubMed: 17889968]

Buckner RL, Snyder AZ, Shannon BJ, LaRossa G, Sachs R, Fotenos AF, Sheline YI, Klunk WE, Mathis CA, Morris JC, Mintun MA. Molecular, structural, and functional characterization of Alzheimer's disease: evidence for a relationship between default activity, amyloid, and memory. J Neurosci 2005;25:7709–7717. [PubMed: 16120771]

Buerger K, Ewers M, Andreasen N, Zinkowski R, Ishiguro K, Vanmechelen E, Teipel SJ, Graz C, Blennow K, Hampel H. Phosphorylated tau predicts rate of cognitive decline in MCI subjects: a comparative CSF study. Neurology 2005;65:1502–1503. [PubMed: 16275849]

Buerger K, Teipel SJ, Zinkowski R, Blennow K, Arai H, Engel R, Hofmann-Kiefer K, McCulloch C, Ptok U, Heun R, Andreasen N, deBernardis J, Kerkman D, Moeller H, Davies P, Hampel H. CSF tau protein phosphorylated at threonine two hundred and thirty-one correlates with cognitive decline in MCI subjects. Neurology 2002;59:627–629. [PubMed: 12196665]

Caselli RJ, Dueck AC, Osborne D, Sabbagh MN, Connor DJ, Ahern GL, Baxter LC, Rapcsak SZ, Shi J, Woodruff BK, Locke DE, Snyder CH, Alexander GE, Rademakers R, Reiman EM. Longitudinal modeling of age-related memory decline and the APOE epsilon4 effect. N Engl J Med 2009;361:255–263. [PubMed: 19605830]

Clark CM, Xie S, Chittams J, Ewbank D, Peskind E, Galasko D, Morris JC, McKeel DW Jr, Farlow M, Weitlauf SL, Quinn J, Kaye J, Knopman D, Arai H, Doody RS, de Carli C, Leight S, Lee VM, Trojanowski JQ. Cerebrospinal fluid tau and beta-amyloid: how well do these biomarkers reflect autopsy-confirmed dementia diagnoses? Arch. Neurol 2003;60:1696–1702.

Collins DL, Neelin P, Peters TM, Evans AC. Automatic 3D intersubject registration of MR volumetric data in standardized Talairach space. J Comput Assist Tomogr 1994;18:192–205. [PubMed: 8126267]

Cosentino S, Scarmeas N, Helzner E, Glymour MM, Brandt J, Albert M, Blacker D, Stern Y. APOE epsilon 4 allele predicts faster cognitive decline in mild Alzheimer disease. Neurology 2008;70:1842–1849. [PubMed: 18401023]

Cummings JL. Defining and labeling disease-modifying treatments for Alzheimer's disease. Alzheimers Dement 2009;5:406–418. [PubMed: 19751920]

de Leon MJ, DeSanti S, Zinkowski R, Mehta PD, Pratico D, Segal S, Rusinek H, Li J, Tsui W, Saint LLA, Clark CM, Tarshish C, Li Y, Lair L, Javier E, Rich K, Lesbre P, Mosconi L, Reisberg B, Sadowski M, deBernadis JF, Kerkman DJ, Hampel H, Wahlund LO, Davies P. Longitudinal CSF and MRI biomarkers improve the diagnosis of mild cognitive impairment. Neurobiol Aging 2006;27:394–401. [PubMed: 16125823]

de Toledo-Morrell L, Dickerson B, Sullivan MP, Spanovic C, Wilson R, Bennett DA. Hemispheric differences in hippocampal volume predict verbal and spatial memory performance in patients with Alzheimer's disease. Hippocampus 2000;10:136–142. [PubMed: 10791835]

Dorfel D, Werner A, Schaefer M, von Kummer R, Karl A. Distinct brain networks in recognition memory share a defined region in the precuneus. Eur J Neurosci 2009;30:1947–1959. [PubMed: 19895564]

Engler H, Forsberg A, Almkvist O, Blomquist G, Larsson E, Savitcheva I, Wall A, Ringheim A, Langstrom B, Nordberg A. Two-year follow-up of amyloid deposition in patients with Alzheimer's disease. Brain 2006;129:2856–2866. [PubMed: 16854944]

Fagan AM, Head D, Shah AR, Marcus D, Mintun M, Morris JC, Holtzman DM. Decreased cerebrospinal fluid Abeta(forty-two) correlates with brain atrophy in cognitively normal elderly. Ann Neurol 2009;65:176–183. [PubMed: 19260027]

Fischl B, Salat DH, Busa E, Albert M, Dieterich M, Haselgrove C, van der Kouwe A, Killiany R, Kennedy D, Klaveness S, Montillo A, Makris N, Rosen B, Dale AM. Whole brain segmentation: automated labeling of neuroanatomical structures in the human brain. Neuron 2002;33:341–355. [PubMed: 11832223]

Fleischman DA, Wilson RS, Gabrieli JD, Schneider JA, Bienias JL, Bennett DA. Implicit memory and Alzheimer's disease neuropathology. Brain 2005;128:2006–2015. [PubMed: 15975947]

Fleisher A, Grundman M, Jack CR Jr, Petersen RC, Taylor C, Kim HT, Schiller DH, Bagwell V, Sencakova D, Weiner MF, de-Carli C, de Kosky ST, van Dyck CH, Thal LJ. Sex, apolipoprotein E epsilon 4 status, and hippocampal volume in mild cognitive impairment. Arch Neurol 2005;62:953–957. [PubMed: 15956166]

Folstein MF, Folstein SE, McHugh PR. Mini-Mental State: a practical method for grading the cogntive state of patients for the clinician. J Psychiatr Res 1975;12:189–198. [PubMed: 1202204]

Frackowiak, RSJ.; Friston, KJ.; Frith, C.; Dolan, R.; Mazziotta, JC., editors. Human Brain Function. Academic Press; 2007.

Freund Y, Shapire R. A decision-theoretic gneralization of online learning and an application to boosting. J Comput Syst Sci 1997;55:119–139.

Frisoni GB, Lorenzi M, Caroli A, Kemppainen N, Nagren K, Rinne JO. In vivo mapping of amyloid toxicity in Alzheimer disease. Neurology 2009a;72:1504–1511. [PubMed: 19398705]

Frisoni GB, Prestia A, Zanetti O, Galluzzi S, Romano M, Cotelli M, Gennarelli M, Binetti G, Bocchio L, Paghera B, Amicucci G, Bonetti M, Benussi L, Ghidoni R, Geroldi C. Markers of Alzheimer's disease in a population attending a memory clinic. Alzheimers Dement 2009b;5:307–317. [PubMed: 19560101]

Galasko D, Chang L, Motter R, Clark CM, Kaye J, Knopman D, Thomas R, Kholodenko D, Schenk D, Lieberburg I, Miller B, Green R, Basherad R, Kertiles L, Boss MA, Seubert P. High cerebrospinal fluid tau and low amyloid beta42 levels in the clinical diagnosis of Alzheimer disease and relation to apolipoprotein E genotype. Arch Neurol 1998;55:937–945. [PubMed: 9678311]

Gunter, J.; Bernstein, M.; Borowski, B.; Felmlee, J.; Blezek, D.; Mallozzi, R. Validation testing of the MRI calibration phantom for the Alzheimer's Disease Neuroimaging Initiative Study. ISMRM 14th Scientific Meeting and Exhibition; 2006.

Hampel H, Burger K, Pruessner JC, Zinkowski R, de Bernadis J, Kerkman D, Leinsinger G, Evans AC, Davies P, Moller HJ, Teipel SJ. Correlation of cerebrospinal fluid levels of tau protein phosphorylated at threonine two hundred and thirty-one with rates of hippocampal atrophy in Alzheimer disease. Arch Neurol 2005;62:770–773. [PubMed: 15883264]

Hampel H, Teipel SJ, Fuchsberger T, Andreasen N, Wiltfang J, Otto M, Shen Y, Dodel R, Du Y, Farlow M, Moller HJ, Blennow K, Buerger K. Value of CSF beta-amyloid1-42 and tau as predictors of Alzheimer's disease in patients with mild cognitive impairment. Mol Psychiatry 2004;9:705–710. [PubMed: 14699432]

Hansson O, Zetterberg H, Buchhave P, Londos E, Blennow K, Minthon L. Association between CSF biomarkers and incipient Alzheimer's disease in patients with mild cognitive impairment: a follow-up study. Lancet Neurol 2006;5:228–234. [PubMed: 16488378]

Hebert LE, Beckett LA, Scherr PA, Evans DA. Annual incidence of Alzheimer disease in the United States projected to the years 2000 through 2050. Alzheimer Dis Assoc Disord 2001;15:169–173. [PubMed: 11723367]

Henneman WJ, Vrenken H, Barnes J, Sluimer IC, Verwey NA, Blankenstein MA, Klein M, Fox NC, Scheltens P, Barkhof F, van der Flier WM. Baseline CSF p-tau levels independently predict progression of hippocampal atrophy in Alzheimer disease. Neurology 2009;73:935–940. [PubMed: 19770469]

Ikonomovic MD, Klunk WE, Abrahamson EE, Mathis CA, Price JC, Tsopelas ND, Lopresti BJ, Ziolko S, Bi W, Paljug WR, Debnath ML, Hope CE, Isanski BA, Hamilton RL, deKosky ST. Post-mortem correlates of in vivo PiB-PET amyloid imaging in a typical case of Alzheimer's disease. Brain 2008;131:1630–1645. [PubMed: 18339640]

Jack CR Jr, Bernstein MA, Fox NC, Thompson P, Alexander G, Harvey D, Borowski B, Britson PJ, Whitwell JL, Ward C, Dale AM, Felmlee JP, Gunter JL, Hill DL, Killiany R, Schuff N, Fox-Bosetti S, Lin C, Studholme C, deCarli CS, Krueger G, Ward HA, Metzger GJ, Scott KT, Mallozzi R, Blezek D, Levy J, Debbins JP, Fleisher AS, Albert M, Green R, Bartzokis G, Glover G, Mugler J, Weiner MW. The Alzheimer's Disease Neuroimaging Initiative (ADNI): MRI methods. J Magn Reson Imaging 2008a;27:685–691. [PubMed: 18302232]

Jack CR Jr, Knopman DS, Jagust WJ, Shaw LM, Aisen PS, Weiner MW, Petersen RC, Trojanowski JQ. Hypothetical model of dynamic biomarkers of the Alzheimer's pathological cascade. Lancet Neurol 2010;9:119–128. [PubMed: 20083042]

Jack CR Jr, Lowe VJ, Senjem ML, Weigand SD, Kemp BJ, Shiung MM, Knopman DS, Boeve BF, Klunk WE, Mathis CA, Petersen RC. 11C PiB and structural MRI provide complementary information in imaging of Alzheimer's disease and amnestic mild cognitive impairment. Brain 2008b;131:665–680. [PubMed: 18263627]

Jack CR Jr, Lowe VJ, Weigand SD, Wiste HJ, Senjem ML, Knopman DS, Shiung MM, Gunter JL, Boeve BF, Kemp BJ, Weiner M, Petersen RC. Serial PIB and MRI in normal, mild cognitive impairment and Alzheimer's disease: implications for sequence of pathological events in Alzheimer's disease. Brain 2009;132:1355–1365. [PubMed: 19339253]

Jack CR Jr, Petersen RC, Xu Y, O'Brien PC, Smith GE, Ivnik RJ, Boeve BF, Tangalos EG, Kokmen E. Rates of hippocampal atrophy correlate with change in clinical status in aging and AD. Neurology 2000;55:484–489. [PubMed: 10953178]

Jack CR Jr, Petersen RC, Xu Y, O'Brien PC, Smith GE, Ivnik RJ, Tangalos EG, Kokmen E. Rate of medial temporal lobe atrophy in typical aging and Alzheimer's disease. Neurology 1998;51:993–999. [PubMed: 9781519]

Jack CR Jr, Petersen RC, Xu YC, Waring SC, O'Brien PC, Tangalos EG, Smith GE, Ivnik RJ, Kokmen E. Medial temporal atrophy on MRI in normal aging and very mild Alzheimer's disease. [see comment]. Neurology 1997;49:786–794. [PubMed: 9305341]

Jicha GA, Parisi JE, Dickson DW, Johnson K, Cha R, Ivnik RJ, Tangalos EG, Boeve BF, Knopman DS, Braak H, Petersen RC. Neuropathologic outcome of mild cognitive impairment following progression to clinical dementia. Arch Neurol 2006;63:674–681. [PubMed: 16682537]

Jovicich J, Czanner S, Greve D, Haley E, van der Kouwe A, Gollub R, Kennedy D, Schmitt F, Brown G, Macfall J, Fischl B, Dale A. Reliability in multi-site structural MRI studies: effects of gradient non-linearity correction on phantom and human data. Neuroimage 2006;30:436–443. [PubMed: 16300968]

Kemppainen NM, Aalto S, Wilson IA, Nagren K, Helin S, Bruck A, Oikonen V, Kailajarvi M, Scheinin M, Viitanen M, Parkkola R, Rinne JO. PET amyloid ligand [11C]PIB uptake is increased in mild cognitive impairment. Neurology 2007;68:1603–1606. [PubMed: 17485647]

Laurens KR, Kiehl KA, Liddle PF. A supramodal limbic-paralimbic-neocortical network supports goal-directed stimulus processing. Hum Brain Mapp 2005;24:35–49. [PubMed: 15593271]

Leow AD, Klunder AD, Jack CR Jr, Toga AW, Dale AM, Bernstein MA, Britson PJ, Gunter JL, Ward CP, Whitwell JL, Borowski BJ, Fleisher AS, Fox NC, Harvey D, Kornak J, Schuff N, Studholme

C, Alexander GE, Weiner MW, Thompson PM. Longitudinal stability of MRI for mapping brain change using tensor-based morphometry. Neuroimage 2006;31:627–640. [PubMed: 16480900]

Mathis CA, Lopresti BJ, Klunk WE. Impact of amyloid imaging on drug development in Alzheimer's disease. Nucl Med Biol 2007;34:809–822. [PubMed: 17921032]

Mattsson N, Zetterberg H, Hansson O, Andreasen N, Parnetti L, Jonsson M, Herukka SK, van der Flier WM, Blankenstein MA, Ewers M, Rich K, Kaiser E, Verbeek M, Tsolaki M, Mulugeta E, Rosen E, Aarsland D, Visser PJ, Schroder J, Marcusson J, de Leon M, Hampel H, Scheltens P, Pirttila T, Wallin A, Jonhagen ME, Minthon L, Winblad B, Blennow K. CSF biomarkers and incipient Alzheimer disease in patients with mild cognitive impairment. JAMA 2009;302:385–393. [PubMed: 19622817]

Mazziotta J, Toga A, Evans A, Fox P, Lancaster J, Zilles K, Woods R, Paus T, Simpson G, Pike B, Holmes C, Collins L, Thompson P, MacDonald D, Iacoboni M, Schormann T, Amunts K, Palomero-Gallagher N, Geyer S, Parsons L, Narr K, Kabani N, Le Goualher G, Boomsma D, Cannon T, Kawashima R, Mazoyer B. A probabilistic atlas and reference system for the human brain: International Consortium for Brain Mapping (ICBM). Philos Trans R Soc Lond B Biol Sci 2001;356:1293–1322. [PubMed: 11545704]

McKhann G, Drachman D, Folstein M, Katzman R, Price D, Stadlan EM. Clinical diagnosis of Alzheimer's disease: report of the NINCDS-ADRDA Work Group under the auspices of Department of Health and Human Services Task Force on Alzheimer's Disease. Neurology 1984;34:939–944. [PubMed: 6610841]

Mintun MA, Larossa GN, Sheline YI, Dence CS, Lee SY, Mach RH, Klunk WE, Mathis CA, deKosky ST, Morris JC. [11C]PIB in a nondemented population: potential antecedent marker of Alzheimer disease. Neurology 2006;67:446–452. [PubMed: 16894106]

Mormino EC, Kluth JT, Madison CM, Rabinovici GD, Baker SL, Miller BL, Koeppe RA, Mathis CA, Weiner MW, Jagust WJ. Episodic memory loss is related to hippocampal-mediated beta-amyloid deposition in elderly subjects. Brain 2009;132:1310–1323. [PubMed: 19042931]

Morra JH, Tu Z, Apostolova LG, Green AE, Avedissian C, Madsen SK, Parikshak N, Hua X, Toga AW, Jack CR Jr, Schuff N, Weiner MW, Thompson PM. Automated 3D mapping of hippocampal atrophy and its clinical correlates in 400 subjects with Alzheimer's disease, mild cognitive impairment, and elderly controls. Hum Brain Mapp 2009;30:2766–2788. [PubMed: 19172649]

Morra JH, Tu Z, Apostolova LG, Green AE, Avedissian C, Madsen SK, Parikshak N, Hua X, Toga AW, Jack CR Jr, Weiner MW, Thompson PM. Validation of a fully automated 3D hippocampal segmentation method using subjects with Alzheimer's disease mild cognitive impairment, and elderly controls. Neuroimage 2008a;43:59–68. [PubMed: 18675918]

Morra JH, Tu Z, Apostolova LG, Green AE, Avedissian C, Madsen SK, Parikshak N, Toga AW, Jack CR Jr, Schuff N, Weiner MW, Thompson PM. Automated mapping of hippocampal atrophy in 1-year repeat MRI data from 490 subjects with Alzheimer's disease, mild cognitive impairment, and elderly controls. Neuroimage 2009;45:S3–15. [PubMed: 19041724]

Morra JH, Tu Z, Apostolova LG, Green A, Toga AW, Thompson PM. Comparison of AdaBoost and support vector machines for detecting Alzheimer's disease through automated hippocampal segmentation. IEEE Trans Med Imaging 2010;29:30–43. [PubMed: 19457748]

Morra JH, Tu Z, Apostolova LG, Green AE, Toga AW, Thompson PM. Automatic subcortical segmentation using a contextual model. Med Image Comput Comput Assist Interv 2008c;11:194–201. [PubMed: 18979748]

Morris JC. The Clinical Dementia Rating (CDR): current version and scoring rules. Neurology 1993;43:2412–2414. [PubMed: 8232972]

Morris JC, Roe CM, Grant EA, Head D, Storandt M, Goate AM, Fagan AM, Holtzman DM, Mintun MA. Pittsburgh Compound B imaging and prediction of progression from cognitive normality to symptomatic Alzheimer disease. Arch Neurol 2009;66:1469–1475. [PubMed: 20008650]

Morris JC, Roe CM, Xiong C, Fagan AM, Goate AM, Holtzman DM, Mintun MA. APOE predicts amyloid-beta but not tau Alzheimer pathology in cognitively normal aging. Ann Neurol 2010;67:122–131. [PubMed: 20186853]

Mortimer JA, Gosche KM, Riley KP, Markesbery WR, Snowdon DA. Delayed recall, hippocampal volume and Alzheimer neuropathology: findings from the Nun Study. Neurology 2004;62:428–432. [PubMed: 14872025]

Mount DL, Ashley AV, Lah JJ, Levey AI, Goldstein FC. Is ApoE epsilon4 associated with cognitive functioning in African Americans diagnosed with Alzheimer Disease? An exploratory study. South Med J 2009;102:890–893. [PubMed: 19668025]

Mueller SG, Schuff N, Raptentsetsang S, Elman J, Weiner MW. Selective effect of Apo e4 on CA3 and dentate in normal aging and Alzheimer's disease using high resolution MRI at 4 T. Neuroimage 2008;42:42–48. [PubMed: 18534867]

Mueller SG, Weiner MW. Selective effect of age, Apo e4, and Alzheimer's disease on hippocampal subfields. Hippocampus 2009;19:558–564. [PubMed: 19405132]

Okello A, Koivunen J, Edison P, Archer HA, Turkheimer FE, Nagren K, Bullock R, Walker Z, Kennedy A, Fox NC, Rossor MN, Rinne JO, Brooks DJ. Conversion of amyloid positive and negative MCI to AD over 3 years: an 11C–PIB PET study. Neurology 2009;73:754–760. [PubMed: 19587325]

Petersen RC, Aisen PS, Beckett LA, Donohue MC, Gamst AC, Harvey DJ, Jack CR Jr, Jagust WJ, Shaw LM, Toga AW, Trojanowski JQ, Weiner MW. Alzheimer's Disease Neuroimaging Initiative (ADNI): clinical characterization. Neurology 2010;74:201–209. [PubMed: 20042704]

Pike KE, Savage G, Villemagne VL, Ng S, Moss SA, Maruff P, Mathis CA, Klunk WE, Masters CL, Rowe CC. Beta-amyloid imaging and memory in non-demented individuals: evidence for preclinical Alzheimer's disease. Brain 2007;130:2837–2844. [PubMed: 17928318]

Ravaglia S, Bini P, Sinforiani E, Franciotta D, Zardini E, Tosca P, Moglia A, Costa A. Cerebrospinal fluid levels of tau phosphorylated at threonine one hundred and eighty-one in patients with Alzheimer's disease and vascular dementia. Neurol Sci 2008;29:417–423. [PubMed: 19011737]

Riemenschneider M, Lautenschlager N, Wagenpfeil S, Diehl J, Drzezga A, Kurz A. Cerebrospinal fluid tau and beta-amyloid forty-two proteins identify Alzheimer disease in subjects with mild cognitive impairment. Arch Neurol 2002;59:1729–1734. [PubMed: 12433260]

Schonheit B, Zarski R, Ohm TG. Spatial and temporal relationships between plaques and tangles in Alzheimer-pathology. Neurobiol Aging 2004;25:697–711. [PubMed: 15165691]

Shaw LM, Vanderstichele H, Knapik-Czajka M, Clark CM, Aisen PS, Petersen RC, Blennow K, Soares H, Simon A, Lewczuk P, Dean R, Siemers E, Potter W, Lee VM, Trojanowski JQ. Cerebrospinal fluid biomarker signature in Alzheimer's disease neuroimaging initiative subjects. Ann Neurol 2009;65:403–413. [PubMed: 19296504]

Sheline YI, Raichle ME, Snyder AZ, Morris JC, Head D, Wang S, Mintun MA. Amyloid plaques disrupt resting state default mode network connectivity in cognitively normal elderly. Biol Psychiatry 2009;67:584–587. [PubMed: 19833321]

Sled JG, Zijdenbos AP, Evans AC. A nonparametric method for automatic correction of intensity nonuniformity in MRI data. IEEE Trans J Med Imaging 1998;17:87–97.

Small GW, Kepe V, Ercoli LM, Siddarth P, Bookheimer SY, Miller KJ, Lavretsky H, Burggren AC, Cole GM, Vinters HV, Thompson PM, Huang SC, Satyamurthy N, Phelps ME, Barrio JR. PET of brain amyloid and tau in mild cognitive impairment. N Engl J Med 2006;355:2652–2663. [PubMed: 17182990]

Storandt M, Mintun MA, Head D, Morris JC. Cognitive decline and brain volume loss as signatures of cerebral amyloid-beta peptide deposition identified with Pittsburgh compound B: cognitive decline associated with Abeta deposition. Arch Neurol 2009;66:1476–1481. [PubMed: 20008651]

Teipel SJ, Bokde AL, Meindl T, Amaro E Jr, Soldner J, Reiser MF, Herpertz SC, Moller HJ, Hampel H. White matter microstructure underlying default mode network connectivity in the human brain. Neuroimage 2009;49:2021–2032. [PubMed: 19878723]

Thompson PW, Ye L, Morgenstern JL, Sue L, Beach TG, Judd DJ, Shipley NJ, Libri V, Lockhart A. Interaction of the amyloid imaging tracer FDDNP with hallmark Alzheimer's disease pathologies. J Neurochem 2009;109:623–630. [PubMed: 19226369]

Tolboom N, van der Flier WM, Yaqub M, Koene T, Boellaard R, Windhorst AD, Scheltens P, Lammertsma AA, van Berckel BN. Differential association of [11C]PIB and [18F]FDDNP binding with cognitive impairment. Neurology 2009;73:2079–2085. [PubMed: 20018636]

van de Pol LA, van der Flier WM, Korf ES, Fox NC, Barkhof F, Scheltens P. Baseline predictors of rates of hippocampal atrophy in mild cognitive impairment. Neurology 2007;69:1491–1497. [PubMed: 17923611]

Visser PJ, Verhey F, Knol DL, Scheltens P, Wahlund LO, Freund-Levi Y, Tsolaki M, Minthon L, Wallin AK, Hampel H, Burger K, Pirttila T, Soininen H, Rikkert MO, Verbeek MM, Spiru L, Blennow K. Prevalence and prognostic value of CSF markers of Alzheimer's disease pathology in patients with subjective cognitive impairment or mild cognitive impairment in the DESCRIPA study: a prospective cohort study. Lancet Neurol 2009;8:619–627. [PubMed: 19523877]

Wallin AK, Blennow K, Andreasen N, Minthon L. CSF biomarkers for Alzheimer's Disease: levels of beta-amyloid, tau, phosphorylated tau relate to clinical symptoms and survival. Dement Geriatr Cogn Disord 2006;21:131–138. [PubMed: 16391474]

Wechsler, D. Wechsler Memory Scale – Revised. Psychological Corporation; San, Antonio, TX: 1987.

Wilson AA, Garcia A, Chestakova A, Kung H, Houle S. A rapid one-step radiosynthesis of beta-amyloid imaging radiotracer N-methyl [11C]2-(4″-methylamonophenyl)-6-hydroxybenzothiazole ([11C]-6-OH-BTA-1). Journal of Labelled Compounds & Radiopharmaceuticals 2004:679–682.

Zarow C, Vinters HV, Ellis WG, Weiner MW, Mungas D, White L, Chui HC. Correlates of hippocampal neuron number in Alzheimer's disease and ischemic vascular dementia. Ann Neurol 2005;57:896–903. [PubMed: 15929035]

Ziolko SK, Weissfeld LA, Klunk WE, Mathis CA, Hoge JA, Lopresti BJ, deKosky ST, Price JC. Evaluation of voxel-based methods for the statistical analysis of PIB PET amyloid imaging studies in Alzheimer's disease. Neuroimage 2006;33:94–102. [PubMed: 16905334]
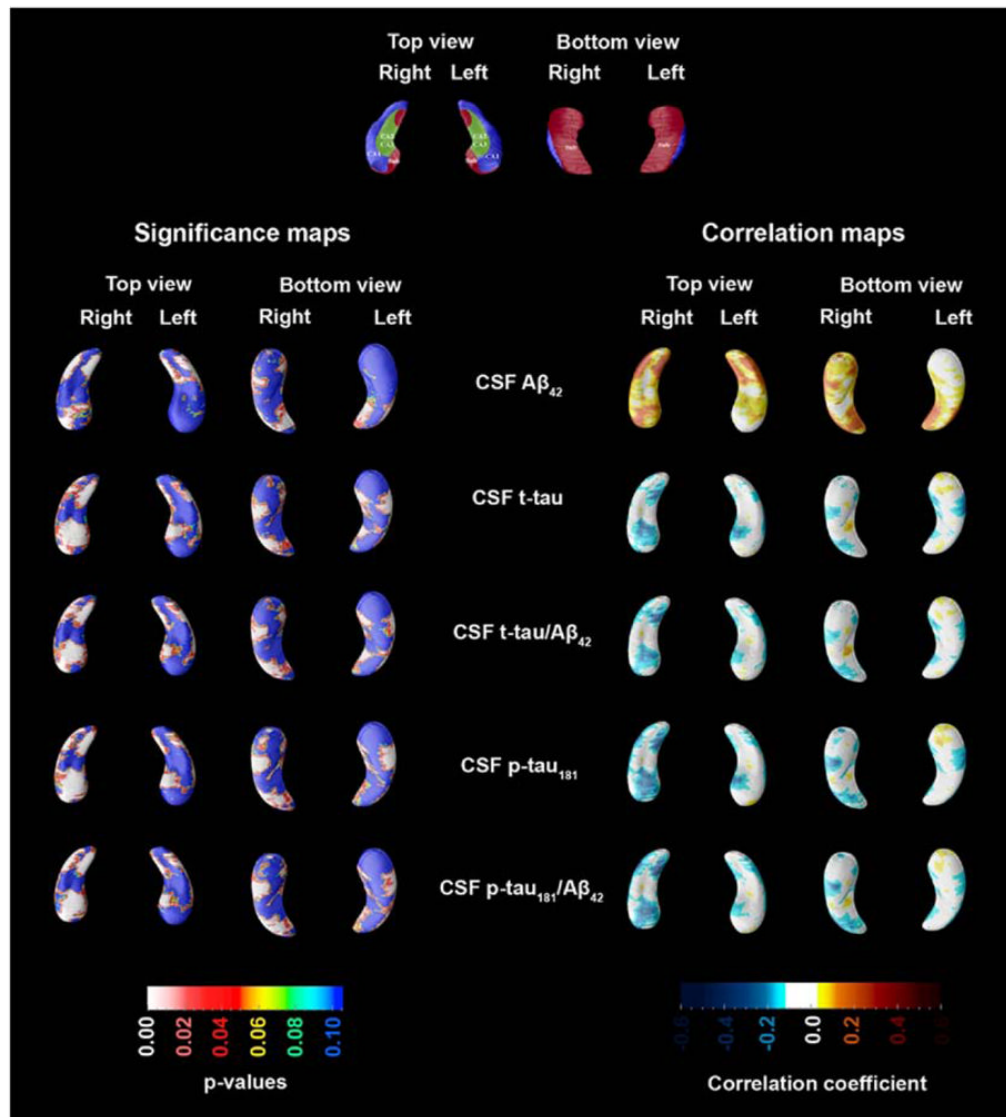
Fig. 1.
Three-dimensional (3D) statistical maps of the associations between cerebrospinal fluid (CSF) biomarkers and hippocampal radial distance (for areas in red and white $p < 0.05$). For permutation corrected significance values see Table 2.
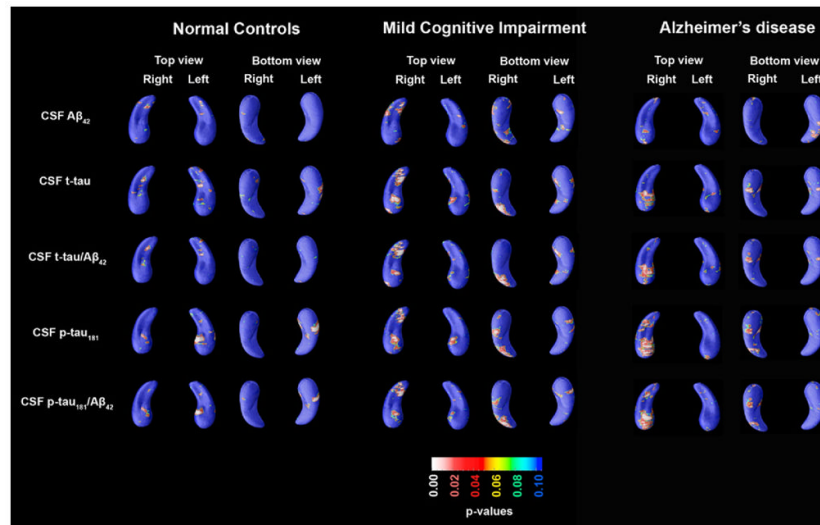
Fig. 2.
Three-dimensional (3D) statistical maps of the associations between cerebrospinal fluid (CSF) biomarkers and hippocampal radial distance in normal control (NC), mild cognitive impairment (MCI), and Alzheimer's disease (AD) (for areas in red and white $p < 0.05$).
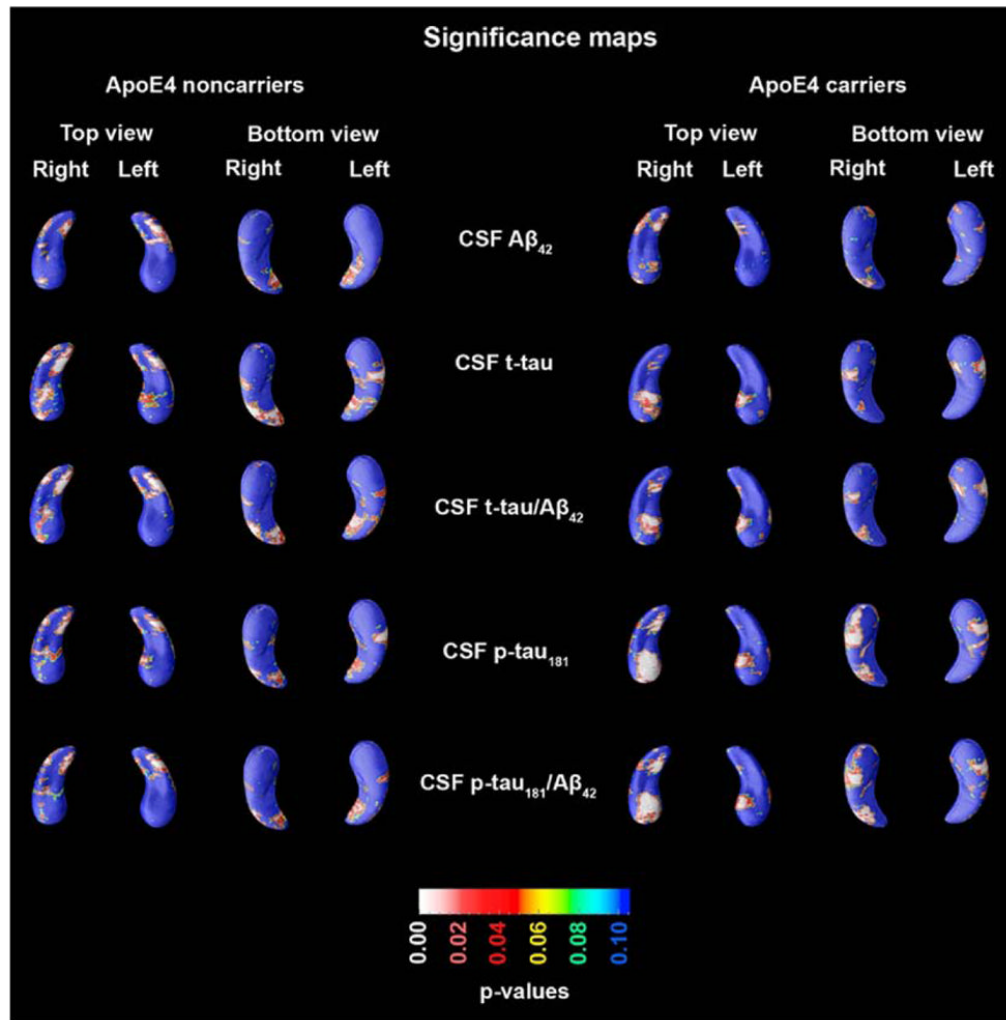
Fig. 3.
Three-dimensional (3D) statistical maps of the associations between cerebrospinal fluid (CSF) biomarkers and hippocampal radial distance in ApoE4 carriers and noncarriers (for areas in red and white $p < 0.05$).
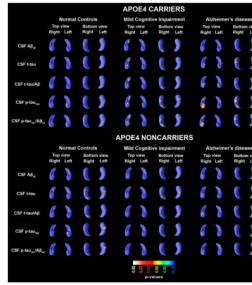
Fig. 4.
Three-dimensional (3D) statistical maps of the associations between cerebrospinal fluid (CSF) biomarkers and hippocampal radial distance in ApoE4 carriers and noncarriers within each diagnostic category (for areas in red and white $p < 0.05$).
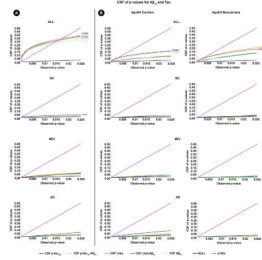
Fig. 5.
Cumulative distribution function (CDF) plots comparing the strengths of the associations between the cerebrospinal fluid (CSF) biomarker measures and hippocampal radial distance in the pooled sample (A) and in each diagnostic group (B). The y = 20× line denotes the threshold that controls the allowed 5% false discovery rate (FDR) (i.e., the maximum proportion of false positives allowed, by convention, for a map to be declared significant overall).
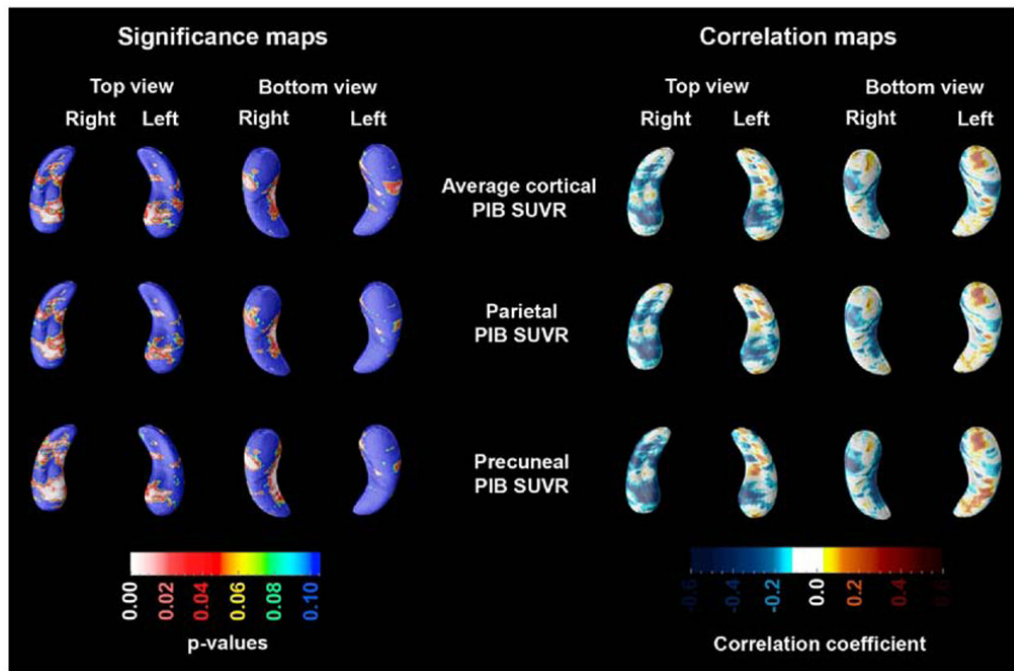
Fig. 6.
Three-dimensional (3D) statistical maps of the associations between the 3 Pittsburgh Compound B (PIB) biomarkers and hippocampal radial distance (for areas in red and white $p < 0.05$).
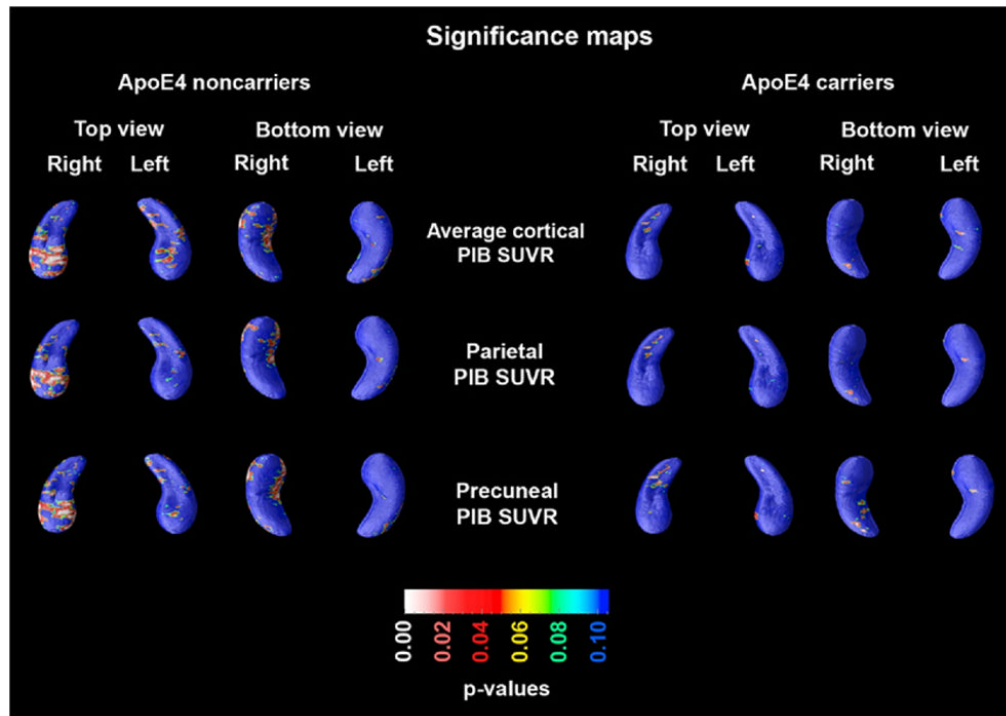
Fig. 7.
Three-dimensional (3D) statistical maps of the associations between Pittsburgh Compound B (PIB) biomarkers and hippocampal radial distance in ApoE4 carriers and noncarriers (for areas in red and white $p < 0.05$).
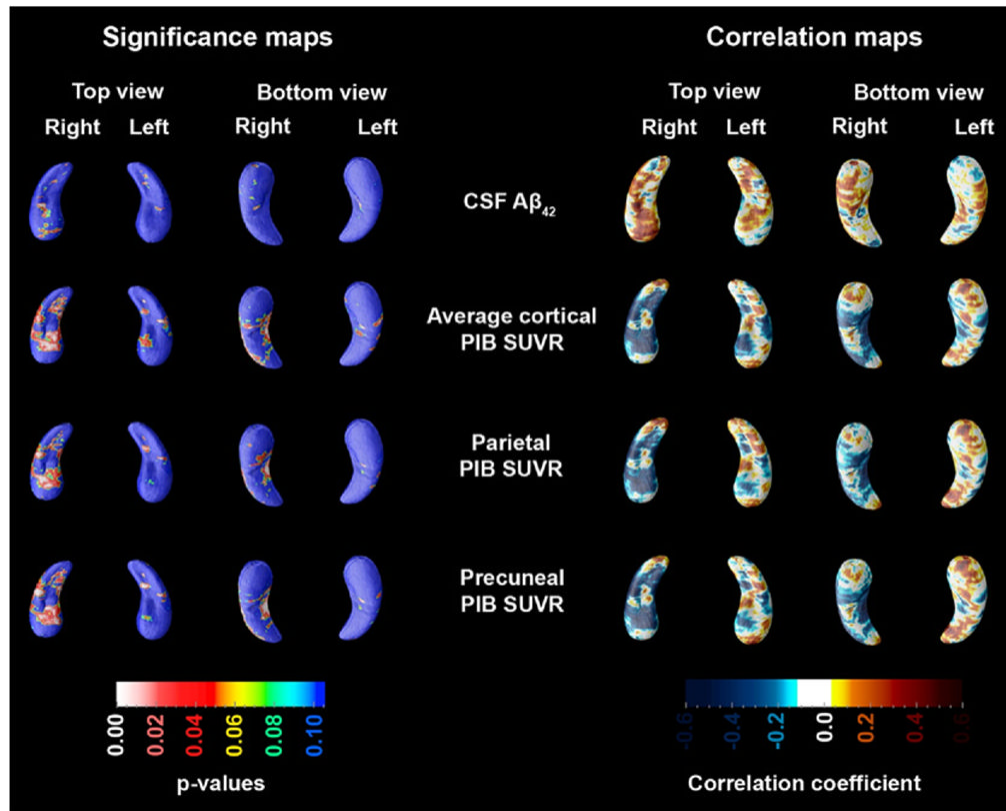
Fig. 8.
Three-dimensional (3D) statistical maps of the associations between cerebrospinal fluid (CSF) amyloid beta (Aβ)$_{42}$ and the 3 Pittsburgh Compound B (PIB) biomarkers and hippocampal radial distance in the combined CSF/PIB sample (for areas in red and white $p < 0.05$).

Table 1

Mean demographic and biomarker data

CSF biomarker sample

Variable at baseline	NC (*n* = 111)	MCI (*n* = 182)	AD (*n* = 95)	All subjects	One-way ANOVA/χ_2 test, *p*-value
Age, years	75.5 (5.2)	74.2 (7.4)	74.6 (7.9)	74.7 (7.0)	0.3
Gender, M:F	56:55	121:61	55:40	166:116	**0.023**
Education, years	15.8 (2.8)	15.8 (3.0)	15.3 (3.0)	15.7 (3.0)	0.3
MMSE	29.1 (1.0)	26.9 (1.8)	23.6 (1.9)	26.7 (2.6)	**< 0.0001**
CSF $A\beta_{42}$ level, pg/mL	206 (55)	163 (55)	143 (40)	170 (57)	**< 0.0001**
CSF t-tau level, pg/mL	69 (30)	103 (61)	124 (58)	98 (57)	**< 0.0001**
CSF p-tau$_{181}$ level, pg/mL	25 (15)	35 (18)	43 (20)	34 (19)	**< 0.0001**

PIB PET sample

Variable at time of PIB scan	NC (*n* = 19)	MCI (*n* = 62)	AD (*n* = 17)	All subjects	One-way ANOVA/χ_2 test, *p*-value
Age, years	77.2 (6.5)	75.4 (8.1)	73.7 (7.7)	75.4 (7.8)	0.4
Gender, M:F	11:8	40:22	12:5	63:35	0.7
Education, years	15.3 (3.3)	16.3 (2.8)	15.4 (2.8)	15.9 (2.9)	0.3
MMSE	28.6 (1.6)	27.2 (2.2)	22 (2.9)	26.5 (3.1)	**< 0.0001**
Parietal PIB SUVR	1.56 (0.4)	1.87 (0.4)	2.0 (0.2)	1.83 (0.4)	**0.002**
Precuneal PIB SUVR	1.61 (0.5)	1.97 (0.5)	2.2 (0.3)	1.94 (0.5)	**0.001**
Average cortical PIB SUVR	1.47 (0.3)	1.68 (0.3)	1.76 (0.2)	1.65 (0.3)	**0.002**

Combined CSF/PIB sample

Variable	NC (*n* = 11)	MCI (*n* = 31)	AD (*n* = 7)	All subjects	One-way ANOVA/χ_2 test, *p*-value
Age at CSF collection, years	75.2 (4.6)	74.1 (7.1)	68.4 (4.6)	73.5 (6.6)	0.08
Age at PIB scan, years	75.5 (7.2)	75.5 (7.2)	71.2 (1.6)	74.7 (6.5)	0.3
Gender, M:F	5:6	22:9	4:3	31:18	0.3
Education, years	16.4 (2.8)	16.5 (3.0)	15.1 (3.4)	16.2 (3.0)	0.6
MMSE at CSF collection	29.3 (1.5)	27.4 (1.5)	23.6 (1.3)	27.2 (2.2)	**< 0.0001**
MMSE at PIB scan	28.6 (1.4)	27.2 (2.3)	21.1 (3.0)	26.6 (3.2)	**< 0.0001**
CSF $A\beta_{42}$ level, pg/mL	175 (48)	161 (55)	128 (32)	159 (52)	0.18

CSF biomarker sample

Variable at baseline	NC ($n = 111$)	MCI ($n = 182$)	AD ($n = 95$)	All subjects	One-way ANOVA/χ_2 test, p-value
Parietal PIB SUVR	1.58 (0.37)	1.93 (0.35)	1.95 (0.24)	1.85 (0.37)	**0.018**
Precuneal PIB SUVR	1.7 (0.39)	2.0 (0.45)	2.15 (0.24)	1.98 (0.44)	**0.043**
Average cortical PIB SUVR	1.49 (0.22)	1.71 (0.24)	1.72 (0.16)	1.66 (0.24)	**0.025**

Data are given as mean (SD) or n. Significant p-values ($p < 0.05$) are bolded.

Key: $A\beta$, amyloid beta; AD, Alzheimer's disease; ANOVA, analysis of variance; CSF, cerebrospinal fluid; F, female; M, male; MCI, mild cognitive impairment; MMSE, Mini Mental State Examination; NC, normal control; PET, positron emission tomography; PIB, Pittsburgh Compound B; p-tau, phosphorylated tau; SUVR, standardized uptake value ratio; t-tau, total tau.

Table 2

Significance of the associations between CSF measures and hippocampal volume and radial distance

CSF biomarker	Hippocampus	Volumetric analyses		3D radial distance analyses
		Pearson's *r*	*p*-value	Permutation corrected *p*-value
Pooled sample (*n* = 388)				
CSF Aβ_{42}	Left	0.11	**0.035**	**0.003**
	Right	0.17	**0.001**	**0.0001**
CSF t-tau	Left	−0.17	**0.001**	**0.00015**
	Right	−0.21	**< 0.0001**	**0.0001**
CSF p-tau$_{181}$	Left	−0.17	**0.001**	**0.0004**
	Right	−0.23	**< 0.0001**	**< 0.0001**
CSF t-tau/Aβ_{42}	Left	−0.17	**0.001**	**0.0006**
	Right	−0.21	**< 0.0001**	**< 0.0001**
CSF p-tau$_{181}$/Aβ_{42}	Left	−0.17	**0.001**	**0.0006**
	Right	−0.23	**< 0.0001**	**< 0.0001**
Normal controls (*n* = 111)				
CSF Aβ_{42}	Left	−0.1	>0.1	>0.1
	Right	0.04	>0.1	>0.1
CSF t-tau	Left	−0.1	>0.1	>0.1
	Right	−0.05	>0.1	>0.1
CSF p-tau$_{181}$	Left	−0.02	>0.1	0.066
	Right	0	>0.1	>0.1
CSF t-tau/Aβ_{42}	Left	0.03	>0.1	>0.1
	Right	−0.04	>0.1	>0.1
CSF p-tau$_{181}$/Aβ_{42}	Left	0.03	>0.1	>0.1
	Right	−0.02	>0.1	>0.1
Mild cognitive impairment (*n* = 182)				
CSF Aβ_{42}	Left	0.02	>0.1	>0.1
	Right	0.01	>0.1	>0.1
CSF t-tau	Left	−0.11	>0.1	>0.1
	Right	−0.14	0.057	**0.043**
CSF p-tau$_{181}$	Left	−0.07	>0.1	>0.1
	Right	−0.12	0.098	>0.1
CSF t-tau/Aβ_{42}	Left	−0.09	>0.1	>0.1
	Right	−0.12	>0.1	**0.042**
CSF p-tau$_{181}$/Aβ_{42}	Left	−0.06	>0.1	>0.1
	Right	−0.12	>0.1	**0.047**
Alzheimer's disease (*n* = 95)				
CSF Aβ_{42}	Left	0.09	>0.1	>0.1
	Right	0.06	>0.1	>0.1
CSF t-tau	Left	−0.01	>0.1	>0.1
	Right	−0.06	>0.1	>0.1

CSF biomarker	Hippocampus	Volumetric analyses		3D radial distance analyses
		Pearson's r	p-value	Permutation corrected p-value
CSF p-tau$_{181}$	Left	−0.1	>0.1	>0.1
	Right	−0.2	**0.02**	0.08
CSF t-tau/Aβ_{42}	Left	−0.06	>0.1	>0.1
	Right	−0.08	>0.1	>0.1
CSF p-tau$_{181}$/Aβ_{42}	Left	−0.12	>0.1	>0.1
	Right	−0.22	**0.036**	>0.1

Key: 3D, 3-dimensional; Aβ, amyloid beta; CSF, cerebrospinal fluid; p-tau, phosphorylated tau; t-tau, total tau.

Table 3

Significance of the associations between CSF measures and hippocampal volume and radial distance in ApoE4 carriers

CSF biomarker	Hippocampus	Volumetric analyses		3D radial distance analyses
		Pearson's *r*	*p*-value	Permutation corrected *p*-value
Pooled sample (*n* = 191)				
CSF Aβ_{42}	Left	0.1	>0.1	>0.1
	Right	0.16	**0.029**	**0.044**
CSF t-tau	Left	−0.11	>0.1	**0.046**
	Right	−0.18	**< 0.011**	>0.1
CSF p-tau$_{181}$	Left	−0.14	0.052	**0.047**
	Right	−0.21	**0.005**	>0.1
CSF t-tau/Aβ_{42}	Left	−0.14	0.051	0.09
	Right	−0.26	**< 0.0001**	**0.002**
CSF p-tau$_{181}$/Aβ_{42}	Left	−0.16	**0.03**	0.1
	Right	−0.26	**< 0.0001**	**0.003**
Normal controls (*n* = 27)				
CSF Aβ_{42}	Left	−0.13	>0.1	>0.1
	Right	0.21	>0.1	>0.1
CSF t-tau	Left	0.11	>0.1	>0.1
	Right	0.02	>0.1	>0.1
CSF p-tau$_{181}$	Left	−0.07	>0.1	>0.1
	Right	0	>0.1	>0.1
CSF t-tau/Aβ_{42}	Left	0.18	>0.1	>0.1
	Right	−0.02	>0.1	>0.1
CSF p-tau$_{181}$/Aβ_{42}	Left	−0.02	>0.1	>0.1
	Right	−0.04	>0.1	>0.1
Mild cognitive impairment (*n* = 99)				
CSF Aβ_{42}	Left	0.08	>0.1	>0.1
	Right	0.08	>0.1	>0.1
CSF t-tau	Left	−0.12	>0.1	>0.1
	Right	−0.16	>0.1	>0.1
CSF p-tau$_{181}$	Left	−0.11	>0.1	>0.1
	Right	−0.19	0.065	>0.1
CSF t-tau/Aβ_{42}	Left	−0.15	>0.1	>0.1
	Right	−0.18	0.073	>0.1
CSF p-tau$_{181}$/Aβ_{42}	Left	−0.14	>0.1	>0.1
	Right	−0.21	**0.04**	0.059
Alzheimer's disease (*n* = 65)				
CSF Aβ_{42}	Left	0.07	>0.1	>0.1
	Right	0.07	>0.1	>0.1
CSF t-tau	Left	0.04	>0.1	>0.1

CSF biomarker	Hippocampus	Volumetric analyses		3D radial distance analyses
		Pearson's r	p-value	Permutation corrected p-value
CSF p-tau$_{181}$	Right	−0.06	>0.1	>0.1
	Left	−0.09	>0.1	>0.1
CSF t-tau/Aβ_{42}	Right	0.34	**0.005**	**0.03**
	Left	−0.02	>0.1	>0.1
CSF p-tau$_{181}$/Aβ_{42}	Right	−0.08	>0.1	>0.1
	Left	−0.1	>0.1	>0.1
	Right	−0.28	**0.025**	>0.1

Key: 3D, 3-dimensional; Aβ, amyloid beta; CSF, cerebrospinal fluid; p-tau, phosphorylated tau; t-tau, total tau.

Table 4

Significance of the associations between CSF measures and hippocampal volume and radial distance in ApoE4 noncarriers

CSF biomarker	Hippocampus	Volumetric analyses		3D radial distance analyses
		Pearson's r	p-value	Permutation corrected p-value
Pooled sample ($n = 197$)				
CSF Aβ_{42}	Left	0.061	>0.1	**0.023**
	Right	0.071	>0.1	**0.038**
CSF t-tau	Left	−0.22	**0.002**	**0.012**
	Right	−0.17	**0.018**	**0.002**
CSF p-tau$_{181}$	Left	−0.17	**0.016**	**0.01**
	Right	−0.13	0.074	**0.004**
CSF t-tau/Aβ_{42}	Left	−0.15	**0.03**	**0.029**
	Right	−0.12	0.1	**0.032**
CSF p-tau$_{181}$/Aβ_{42}	Left	−0.13	0.061	>0.1
	Right	−0.1	>0.1	>0.1
Normal controls ($n = 84$)				
CSF Aβ_{42}	Left	−0.08	>0.1	>0.1
	Right	0.06	>0.1	>0.1
CSF t-tau	Left	−0.2	0.066	>0.1
	Right	−0.1	>0.1	>0.1
CSF p-tau$_{181}$	Left	−0.03	>0.1	>0.1
	Right	−0.04	>0.1	>0.1
CSF t-tau/Aβ_{42}	Left	−0.08	>0.1	>0.1
	Right	−0.12	>0.1	>0.1
CSF p-tau$_{181}$/Aβ_{42}	Left	0.01	>0.1	>0.1
	Right	−0.08	>0.1	>0.1
Mild cognitive impairment ($n = 83$)				
CSF Aβ_{42}	Left	−0.07	>0.1	>0.1
	Right	−0.1	>0.1	>0.1
CSF t-tau	Left	−0.12	>0.1	>0.1
	Right	−0.08	>0.1	>0.1
CSF p-tau$_{181}$	Left	−0.05	>0.1	>0.1
	Right	−0.002	>0.1	>0.1
CSF t-tau/Aβ_{42}	Left	−0.02	>0.1	>0.1
	Right	−0.002	>0.1	>0.1
CSF p-tau$_{181}$/Aβ_{42}	Left	0.05	>0.1	>0.1
	Right	0.06	>0.1	>0.1
Alzheimer's disease ($n = 30$)				
CSF Aβ_{42}	Left	0.1	>0.1	>0.1
	Right	−0.08	>0.1	>0.1
CSF t-tau	Left	−0.11	>0.1	>0.1

CSF biomarker	Hippocampus	Volumetric analyses		3D radial distance analyses
		Pearson's r	p-value	Permutation corrected p-value
	Right	−0.08	>0.1	>0.1
CSF p-tau$_{181}$	Left	−0.13	>0.1	>0.1
	Right	−0.04	>0.1	>0.1
CSF t-tau/Aβ_{42}	Left	−0.14	>0.1	>0.1
	Right	−0.02	>0.1	>0.1
CSF p-tau$_{181}$/Aβ_{42}	Left	−0.16	>0.1	>0.1
	Right	0.02	>0.1	>0.1

Key: 3D, 3-dimensional; Aβ, amyloid beta; CSF, cerebrospinal fluid; p-tau, phosphorylated tau; t-tau, total tau.

Table 5

Significance of the associations between PIB measures and hippocampal volume and radial distance

CSF biomarker	Hippocampus	Volumetric analyses		3D radial distance analyses
		Pearson's *r*	*p*-value	Permutation corrected *p*-value
Mean cortical SUVR	Left	−0.24	**0.019**	>0.1
	Right	−0.23	**0.028**	**0.097**
Parietal SUVR	Left	−0.2	**0.049**	0.3
	Right	−0.24	**0.022**	>0.1
Precuneal SUVR	Left	−0.21	**0.039**	>0.1
	Right	−0.26	**0.011**	**0.013**

Key: 3D, 3-dimensional; CSF, cerebrospinal fluid; SUVR, standardized uptake value ratio.

Table 6

Significance of the associations between PIB measures and hippocampal volume and radial distance in ApoE4 carriers and noncarriers

CSF biomarker	Hippocampus	Volumetric analyses		3D radial distance analyses
		Pearson's *r*	*p*-value	Permutation corrected *p*-value
ApoE4 carriers				
Mean cortical SUVR	Left	−0.05	0.7	0.8
	Right	−0.5	0.7	0.7
Parietal SUVR	Left	−0.03	0.9	0.6
	Right	−0.04	0.8	0.7
Precuneal SUVR	Left	−0.04	0.8	0.7
	Right	−0.04	0.8	0.4
ApoE4 noncarriers				
Mean cortical SUVR	Left	−0.26	0.074	0.5
	Right	−0.35	**0.018**	0.094
Parietal SUVR	Left	−0.17	0.26	0.7
	Right	−0.32	**0.03**	0.2
Precuneal SUVR	Left	−0.19	0.2	0.6
	Right	−0.35	**0.016**	**0.049**

Key: 3D, 3-dimensional; CSF, cerebrospinal fluid; PIB, Pittsburgh Compound B; SUVR, standardized uptake value ratio.

Table 7

Bivariate Pearson's correlation coefficients between the CSF and PIB biomarkers and hippocampal volume from the combined CSF/PIB dataset ($n = 49$)

CSF biomarker	Hippocampus	Volumetric analyses Pearson's r
CSF Aβ_{42}	Left	0.004
	Right	0.045
CSF t-tau	Left	−0.19
	Right	−0.14
CSF p-tau$_{181}$	Left	−0.26[a]
	Right	−0.24
Precuneal PIB SUVR	Left	−0.07
	Right	−0.22
Parietal PIB SUVR	Left	−0.1
	Right	−0.22
Average cortical PIB SUVR	Left	−0.16
	Right	−0.24[b]

Key: Aβ, amyloid beta; CSF, cerebrospinal fluid; PIB, Pittsburgh Compound B; p-tau, phosphorylated tau; SUVR, standardized uptake value ratio; t-tau, total tau.

[a] $p = 0.069$.

[b] $p = 0.097$.